DISSERTATIONS IN
HEALTH SCIENCES

Jussi Ryynänen

Pleiotropy of Vitamin D-Mediated Gene Regulation

Publications of the University of Eastern Finland
Dissertations in Health Sciences

UNIVERSITY OF
EASTERN FINLAND

JUSSI RYYNÄNEN

Pleiotropy of Vitamin D-Mediated Gene Regulation

To be presented by permission of the Faculty of Health Sciences,
University of Eastern Finland for public examination in Auditorium L21, Snellmania, Kuopio,
on Friday, June 27th 2014, at 12 noon

Publications of the University of Eastern Finland
Dissertations in Health Sciences
237

Institute of Biomedicine, School of Medicine, Faculty of Health Sciences,
University of Eastern Finland
Kuopio
2014

Juvenes Print - Suomen Yliopistopaino Oy
Tampere, 2014

Distributor:
University of Eastern Finland
Kuopio Campus Library
P.O.Box 1627
FI-70211 Kuopio, Finland
http://www.uef.fi/kirjasto

ISBN (print): 978-952-61-1495-8
ISBN (pdf): 978-952-61-1496-5
ISSN (print): 1798-5706
ISSN (pdf): 1798-5714
ISSN-L: 1798-5706

Author's address: Institute of Biomedicine, School of Medicine
University of Eastern Finland
KUOPIO
FINLAND

Supervisors: Professor Carsten Carlberg, Ph.D.
Institute of Biomedicine, School of Medicine
University of Eastern Finland
KUOPIO
FINLAND

Docent Sami Heikkinen, Ph.D.
Institute of Biomedicine, School of Medicine
University of Eastern Finland
KUOPIO
FINLAND

Docent Sami Väisänen, Ph.D.
Roche Diagnostics Oy
ESPOO
FINLAND

Reviewers: Professor Enikö Kállay, Ph.D.
Department of Pathophysiology and Allergy Research
Medical University of Vienna
VIENNA
AUSTRIA

Professor Alberto Muñoz, Ph.D.
Department of Cancer Biology
Instituto de Investigaciones Biomedicas
MADRID
SPAIN

Opponent: Professor Dieter Steinhilber, Ph.D.
Institute of Pharmaceutical Chemistry
Goethe University Frankfurt
FRANKFURT
GERMANY

Ryynänen, Jussi
Pleiotropy of Vitamin D-Mediated Gene Regulation
University of Eastern Finland, Faculty of Health Sciences
Publications of the University of Eastern Finland. Dissertations in Health Sciences 237. 2014. 52 p.

ISBN (print): 978-952-61-1495-8
ISBN (pdf): 978-952-61-1496-5
ISSN (print): 1798-5706
ISSN (pdf): 1798-5714
ISSN-L: 1798-5706

ABSTRACT

The steroid hormone 1,25-dihydroxyvitamin D_3 ($1,25(OH)_2D_3$) is the active metabolite of vitamin D_3 that regulates the transcription of hundreds of primary target genes in many human tissues. $1,25(OH)_2D_3$ mediates its actions through the transcription factor vitamin D receptor (VDR), for which now genome-wide binding data is available. For understanding the physiological impact of the hormone, tissue-specific locations of the VDR, central $1,25(OH)_2D_3$ target genes and the detailed mechanisms of $1,25(OH)_2D_3$-mediated transcriptional regulation needs to be elucidated. In this thesis, the regulatory mechanisms and the central VDR binding loci were characterized in detail, in order to provide more insight into the transcriptional regulation by vitamin D. The dynamic nature of VDR-mediated gene regulation was demonstrated at the example of the *IGFBP3* gene using non-malignant human breast epithelial cells. Furthermore, the genomic regions containing the primary VDR target genes *G0S2*, *CDKN1A*, *MYC*, *CXCL8* and *ASAP2*, which are associated with both immune and cell growth-related functions, were studied in human monocyte and macrophage models. The cancer-associated $1,25(OH)_2D_3$ targets *G0S2*, *CDKN1A* and *MYC* are located in chromosomal regions containing one to four VDR binding sites suggesting an individual regulatory scenario for the each target gene. The gene for the chemotactic cytokine CXCL8 is located in a cluster with eight other *CXCL* genes and is controlled by one prominent VDR binding site both in monocytes and macrophages. In contrast, the chromosomal domain containing the primary $1,25(OH)_2D_3$ target gene *ASAP2* includes three VDR binding sites but only one target gene. In addition, the genes *DUSP10*, *TRAK1*, *NRIP1* and *THBD*, which belong to a short list of genes with conserved VDR binding loci, were studied in a human pre-adipocyte model. Gene expression patterns of these conserved $1,25(OH)_2D_3$ target genes were evaluated in primary human adipose tissue samples from participants of a 5 month vitamin D intervention trial (VitDmet). The expression of the *DUSP10* gene was highlighted as the most suitable biomarker representing the vitamin D status of human individuals. The results of this doctoral thesis emphasize the pleiotropic effects of $1,25(OH)_2D_3$ and provide further insight into the regulation of its primary target genes in human tissues and cell types.

National Library of Medicine Classification: QU 460, QU 56, QU 173, QU 475
Medical Subject Headings: Genomics; Epigenomics; Genetic Pleiotropy; Chromatin; Vitamin D; Calcitriol; Receptors, Calcitriol; Gene Expression Regulation; Transcription, Genetic; Transcription Factors; Monocytes; Macrophages; Adipose Tissue; Biological Markers

Ryynänen, Jussi
D-vitamiinivälitteisen geenien säätelyn pleiotropia
Itä-Suomen yliopisto, terveystieteiden tiedekunta
Publications of the University of Eastern Finland. Dissertations in Health Sciences 237. 2014. 52 s.

ISBN (print): 978-952-61-1495-8
ISBN (pdf): 978-952-61-1496-5
ISSN (print): 1798-5706
ISSN (pdf): 1798-5714
ISSN-L: 1798-5706

TIIVISTELMÄ

Steroidihormoni 1,25-dihydroksivitamiini D_3 ($1,25(OH)_2D_3$) on D_3-vitamiinin aktiivinen metaboliitti, joka säätelee suoraan satojen kohdegeenien transkriptiota useissa ihmiskudoksissa. $1,25(OH)_2D_3$ välittää vaikutuksensa transkriptiotekijä D-vitamiinireseptorin (VDR) kautta, jonka genominlaajuisista sitoutumispaikoista on jo selvityksiä. Jotta $1,25(OH)_2D_3$:n fysiologiset vaikutukset ymmärrettäisiin paremmin, tarvitaan enemmän tietoa VDR:n kudoskohtaisista genomisista sitoutumispaikoista, keskeisistä $1,25(OH)_2D_3$ kohdegeeneistä sekä mekanismeista, joiden välityksellä $1,25(OH)_2D_3$ säätelee transkriptiota. Tässä väitöskirjatutkimuksessa tutkittiin yksityiskohtaisesti VDR:n keskeisiä sitoutumisalueita ja säätelymekanismeja lisätäksemme tietämystä D-vitamiinin välittämästä transkriptionaalisesta säätelystä. Käyttämällä esimerkkinä *IGFBP3*-geeniä hyvälaatuisissa rintarauhassoluissa osoitettiin VDR:n välittämän geenien säätelyn olevan dynaaminen prosessi. Lisäksi tutkittiin ihmisen monosyytti- ja makrofaagimalleissa genomisia alueita, joissa sijaitsevat immuniteettiin ja solukasvuun liittyvät geenit *G0S2*, *CDKN1A*, *MYC*, *CXCL8* ja *ASAP2*. Syöpään yhdistetyt $1,25(OH)_2D_3$:n kohdegeenit *G0S2*, *CDKN1A* ja *MYC* sijaitsevat kromosomaalisilla alueilla, jotka sisältävät yhdestä neljään VDR:n sitoutumispaikkaa. Havainto osoittaa, että jokainen näistä kohdegeeneistä on erityyppisen $1,25(OH)_2D_3$:n välittämän säätelyn alaisena. Kemotaktista sytokiinia CXCL8:aa koodaava geeni sijaitsee ryhmittymässä kahdeksan muun *CXCL*-geenin kanssa, ja sitä säätelee yksi voimakas VDR:n sitoutumispaikka sekä monosyyteissä että makrofaageissa. Sitä vastoin kromosomaalinen alue, joka käsittää $1,25(OH)_2D_3$:n kohdegeenin *ASAP2*:n, sisältää kolme VDR:n sitoutumiskohtaa mutta vain yhden kohdegeenin. Lopuksi tutkittiin ihmisen preadiposyyttimallissa *DUSP10*, *TRAK1*, *NRIP1* ja *THBD* -geenejä, jotka kuuluvat pieneen joukkoon geenejä, joita säätelevät konservoituneet VDR:n sitoutumispaikat. Näiden $1,25(OH)_2D_3$-kohdegeenien ilmentymistasoja mitattiin rasvakudosnäytteistä, jotka oli kerätty kliinisen D-vitamiinin seurantatutkimuksen (VitDmet) osallistujilta. *DUSP10*-geenin ilmentyminen osoittautui sopivimmaksi biomarkkeriksi kuvaamaan yksilöllistä D-vitamiinistatusta elimistössä. Tämän väitöskirjatyön tulokset korostavat $1,25(OH)_2D_3$:n pleiotrooppisia vaikutuksia ja lisäävät tietämystä $1,25(OH)_2D_3$:n ensisijaisten kohdegeenien säätelystä eri ihmiskudoksissa ja ihmissolutyypeissä.

Luokitus: QU 460, QU 56, QU 173, QU 475
Yleinen suomalainen asiasanasto: geenit; geenieksPressio; säätely; genomiikka; epigenetiikka; D-vitamiini; kalsitrioli; reseptorit; valkosolut; makrofagit; rasvakudokset; markkerit

Acknowledgements

This study was carried out at the Institute of Biomedicine, University of Eastern Finland. I wish to express my deepest gratitude to my principal supervisor Professor Carsten Carlberg for all the excellent scientific guidance and the support during the thesis project. His knowledge and passion in research has created such a motivating educational environment to conduct this thesis work.

I am deeply grateful to my supervisor Docent Sami Heikkinen for sharing his knowledge of genome-wide analyses. I am also very thankful for my supervisor Docent Sami Väisänen for his valuable technical advises and rich conversations.

I express my gratitude to the official reviewers, Professor Enikő Kállay and Professor Alberto Muñoz, for the careful review of my thesis and the valuable comments that helped me to improve the work. I wish to thank Dr. Tom Dunlop for critical reading and linquistic correction of my thesis.

I thank all co-authors for their contribution to make this work possible. Especially, I owe my gratitude to Dr. Sabine Seuter for sharing all the technical advises during the main research projects, to Dr. Marjo Malinen for the invaluable advises during the start of my scientific career and to Dr. Antonio Neme for the valuable contribution analyzing sequencing data. I also owe my gratitude to all the current and former members of our research team for sharing their knowledge, for the cheerful discussions and for nice coffee breaks.

I want to thank all my friends and former study mates for bringing the important counterweight for the science.

My warmest thanks go to my parents for giving me all their support and the opportunity to focus on my studies. Especial thanks belong to all my siblings, particularly to my brother Mikko for the encouragement and to my twin sister Hanna, whose very special dogs always cheer me up.

Finally, I want to express the greatest appreciation to Eveliina, who has been great support for me during these years. Our perfect understanding of each other has created such strength for our everyday life.

Kuopio, June 2014

Jussi Ryynänen.

x

List of the original publications

This dissertation is based on the following original publications:

I Malinen M, Ryynänen J, Heinäniemi M, Väisänen S and Carlberg C. Cyclical regulation of the insulin-like growth factor binding protein 3 gene in response to 1α,25-dihydroxyvitamin D_3. *Nucleic Acids Res 39: 502-512, 2011.*

II Ryynänen J, Seuter S, Campbell MJ and Carlberg C. Gene regulatory scenarios of primary 1,25-dihydroxyvitamin D_3 target genes in a human myeloid leukemia cell line. *Cancers 5: 1221-1241, 2013.*

III Ryynänen J and Carlberg C. Primary 1,25-dihydroxyvitamin D_3 response of the interleukin 8 gene cluster in human monocyte- and macrophage-like cells. *PLoS One 8: e78170, 2013.*

IV Seuter S*, Ryynänen J* and Carlberg C. The *ASAP2* gene is a primary target of 1,25-dihydroxyvitamin D_3 in human monocytes and macrophages. *J Steroid Biochem Mol Biol, in press, 2014.*

*) Equal contribution

V Ryynänen J, Neme A, Tuomainen TP, Virtanen JK, Voutilainen S, Nurmi T, de Mello VD, Uusitupa M and Carlberg C. Changes in vitamin D target gene expression in adipose tissue monitor the vitamin D response of human individuals. *Mol Nutr Food Res, accepted, 2014.*

Contents

Abbreviations

$1,25(OH)_2D_3$	1,25-dihydroxyvitamin D_3
$25(OH)D_3$	25-hydroxyvitamin D_3
ASAP2	ArfGAP with SH3 domain, ankyrin repeat and PH domain 2
CDK	cyclin-dependent kinase
CDKI	CDK inhibitor
CDKN1A	cyclin-dependent kinase inhibitor 1A
CD14	cluster of differentiation 14
ChIA-PET	chromatin interaction analysis with paired-end tag sequencing
ChIP	chromatin immunoprecipitation
ChIP-seq	ChIP-sequencing
CTCF	CCCTC-binding factor
CXCL	chemokine CXC motif ligand
CYP24A1	cytochrome P450, family 24, subfamily A, polypeptide 1
DBD	DNA-binding domain
DUSP10	dual specificity phosphatase 10
DR3	direct repeat spaced by 3 nucleotides
FBS	fetal bovine serum
FAIRE	formaldehyde-assisted isolation of regulatory elements
FAIRE-seq	FAIRE-sequencing
G0S2	G_0/G_1 switch 2
H3K4me	histone 3 lysine 4 methylation
HDAC	histone deacetylase
HUVEC	human umbilical vein endothelial cells
IFN-γ	interferon-γ
IGF	insulin-like growth factor
IGFBP	insulin-like growth factor binding protein
IL	interleukin

IκBα	NF-κB inhibitor
LBD	ligand-binding domain
LBP	ligand-binding pocket
LPS	lipopolysaccharide
MYC	v-myc avian myelocytomatosis viral oncogene homolog
NF-κB	nuclear factor-κB
NR	nuclear receptor
NRIP1	nuclear receptor interacting protein 1
NHEK	normal human epidermal keratinocytes
PBMC	peripheral blood mononuclear cell
PBS	phosphate buffered saline
qPCR	real-time quantitative polymerase chain reaction
PMA	phorbol 12-myristate 13-acetate
PTH	parathyroid hormone
RXR	retinoid X receptor
SGBS	Simpson-Golabi-Behmel syndrome
siRNA	small interfering RNA
TGF-β	transforming growth factor-β
THBD	thrombomodulin
TLR	Toll-like receptor
TRAK1	trafficking protein, kinesin binding 1
TSS	transcription start site
UVB	ultraviolet B
VDR	vitamin D receptor

1 Introduction

Vitamin D_3 is the precursor of the biologically most active vitamin D metabolite, 1,25-dihydroxyvitamin D_3 ($1,25(OH)_2D_3$). Despite its name, vitamin D_3 can be synthetized in the skin using the energy of ultraviolet B (UVB) radiation from the sun. Vitamin D_3 production in the skin may not be adequate to maintain proper vitamin D status, due to the seasonal lack of sunlight at higher latitude and/or personal lifestyle. This is a common problem as epidemiological studies, analyzing circulating levels of the storage form of vitamin D, 25-hydroxyvitamin D_3 ($25(OH)D_3$), have revealed that a low vitamin D status may affect more than one-third of the global population (1).

The main physiological role of $1,25(OH)_2D_3$ is to maintain calcium homeostasis, in order to prevent bone loss (2). In addition, epidemiological evidence suggests that functional vitamin D signaling may protect against various diseases, including cancers, autoimmune diseases and even the risk of all-cause death (3). However, epidemiological studies have not provided a mechanistic explanation for the protective role of vitamin D. Therefore, more insight into the molecular actions of $1,25(OH)_2D_3$ is needed in order to better appreciate the physiological impact of the hormone.

All biological actions of $1,25(OH)_2D_3$ are mediated through the vitamin D receptor (VDR) in the nucleus. VDR is a transcription factor and a member of the nuclear receptor (NR) superfamily that binds directly to genomic DNA and is activated through the high affinity binding of $1,25(OH)_2D_3$. Binding leads to transcriptional activation and rapid changes in mRNA levels of primary VDR target genes. Thus, understanding the physiological effects of $1,25(OH)_2D_3$ requires knowledge on genomic VDR binding loci and the genes that are regulated by VDR. Furthermore, in each $1,25(OH)_2D_3$ target tissue, VDR binds to thousands of genomic regions. Thus, $1,25(OH)_2D_3$ has the potential to regulate directly multiple tissue-specific target genes.

A number of primary $1,25(OH)_2D_3$ target genes have been identified to be involved in the regulation of a wide range of physiological functions in different human tissues. For example, $1,25(OH)_2D_3$ regulates immuno-modulatory cytokines, transcription factors and the genes controlling cellular growth. This emphasizes the pleiotropic nature of the hormone. However, recent studies of genome-wide VDR binding sites have revealed thousands of new genomic VDR binding sites with unknown impact on gene regulation. In addition, already known $1,25(OH)_2D_3$ target genes may be regulated by far more distant VDR binding sites than previously estimated.

This doctoral thesis was carried out to extend our understanding of the mechanistic basis and gene regulatory scenarios of VDR-mediated gene regulation. The study revealed mechanistic differences between $1,25(OH)_2D_3$ and its synthetic analog, Gemini, in VDR-mediated gene regulation in non-malignant human breast epithelial cells. In a human monocytic cell line, several genomic regions and primary $1,25(OH)_2D_3$ target genes, which are involved in the control of cellular growth and immune function, were characterized in detail. Finally, cross tissue conserved $1,25(OH)_2D_3$ target genes were studied in adipocytes demonstrating the possibility to use these genes as biomarkers for the actions of vitamin D_3 in human individuals.

2 Review of the Literature

2.1 VITAMIN D METABOLISM

2.1.1 Sources and metabolism

The secosteroid vitamin D_3 is a biologically inactive precursor from which the actual hormone, $1,25(OH)_2D_3$, also known as calcitriol, is derived. Vitamin D_3 is synthetized, when the skin is exposed to sunlight. Then the energy of UVB radiation converts in a multistep process 7-dehydrocholesterol into vitamin D_3. In addition, vitamin D can be obtained from diet, mainly from animal origin, such as fatty fish, liver, eggs or fortified dairy products, or from dietary supplements. Vitamin D_3 can be stored in the liver and in adipose tissue and is released when it is not adequately produced or obtained from diet (4). Vitamin D_2, also known as ergocalciferol, is a form of vitamin D that is obtained only from dietary sources, mainly from plants and fungi. Vitamin D_2 is biologically less active than vitamin D_3. Due to limited dietary sources of vitamin D_2, the main vitamin D form in humans and other animals is vitamin D_3 (4,5).

Two hydroxylation steps are needed for the synthesis of the biologically active form of vitamin D_3. First, vitamin D_3 is 25-hydroxylated, mainly in the liver by the cytochrome P450 (CYP) enzymes CYP27A1 or CYP2R1, to yield $25(OH)D_3$ (6). $25(OH)D_3$ is an inactive form of vitamin D_3 and its serum levels are often used to determine and monitor the vitamin D status of human individuals (7). $25(OH)D_3$ is hydroxylated by the 1α-hydroxylase enzyme CYP27B1, to yield $1,25(OH)_2D_3$, which is the active hormone and responsible for the physiological actions of vitamin D_3 (6). All vitamin D metabolites are transported in the circulation bound to the vitamin D-binding protein. The hydroxylation of $25(OH)D_3$ to $1,25(OH)_2D_3$ occurs mainly in the kidneys and is tightly regulated by parathyroid hormone (PTH). In addition, extra-renal CYP27B1 activity is mediating tissue-specific and intracellular increase in $1,25(OH)_2D_3$ levels. Inactivation of both $1,25(OH)_2D_3$ and $25(OH)D_3$ is achieved by 24-hydroxylation, carried out by the cytochrome P450, family 24, subfamily A, polypeptide 1 (CYP24A1) enzyme, and results in the metabolites $1,24,25(OH)_3D_3$ and $24,25(OH)_2D_3$, respectively. These metabolites are after multiple hydroxylation steps degraded into the water-soluble inactive compounds calcitroic acid or a 26,23-lactone.

In summary, the renal ratio of the activating CYP27B1 and inactivating CYP24A1 enzymes determines systemic $1,25(OH)_2D_3$ and $25(OH)D_3$ levels, whilst tissue-specific CYP24A1 together with CYP27B1 regulates local $1,25(OH)_2D_3$ levels. In addition, CYP24A1 is the rate-limiting enzyme for $1,25(OH)_2D_3$ concentrations, since the *CYP24A1* gene expression is strongly induced by $1,25(OH)_2D_3$ in multiple tissues. All steps of the metabolic cascade are presented in Figure 1.

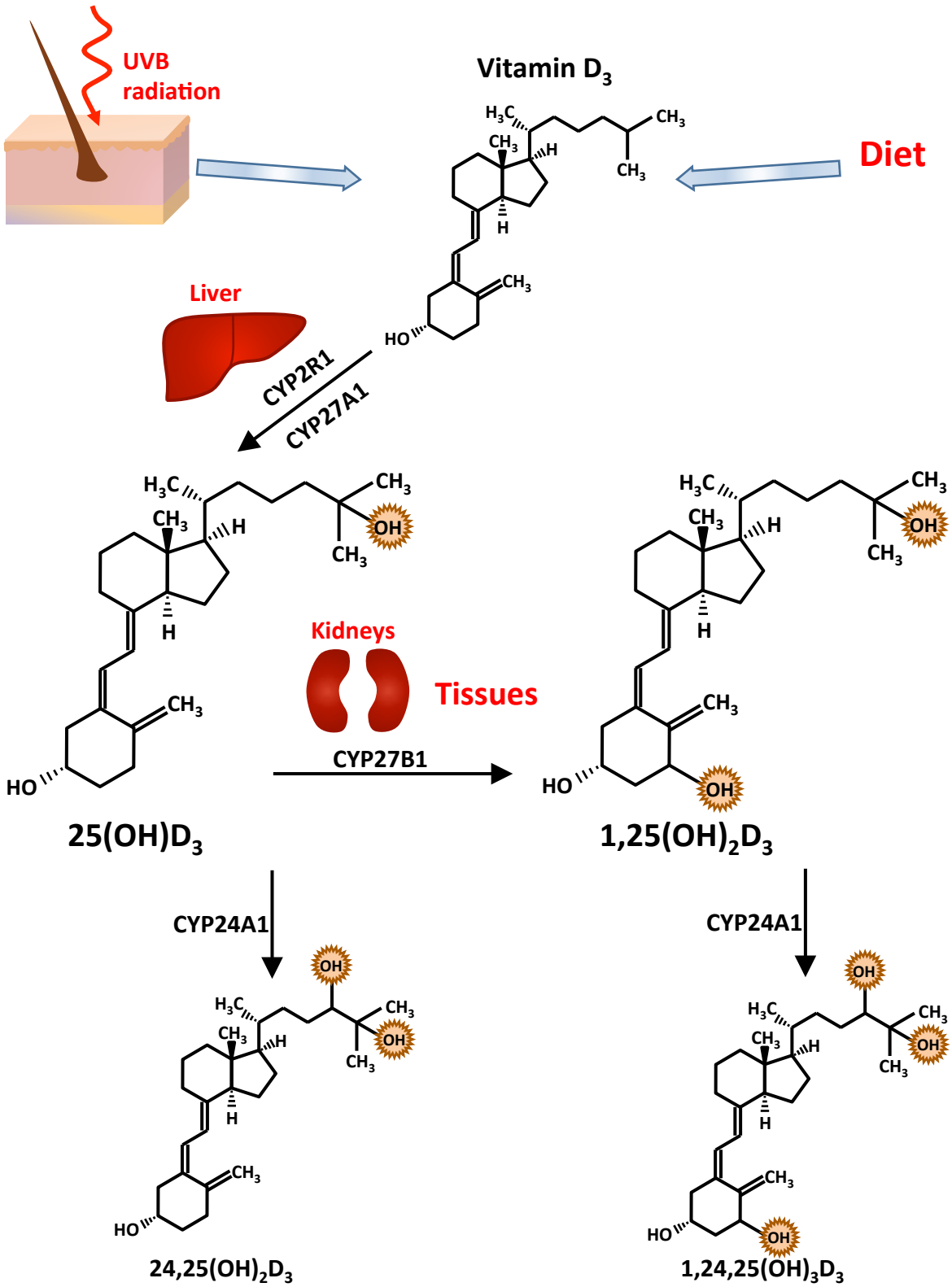

Figure 1. Vitamin D_3 metabolism. Vitamin D_3 is converted to the inactive circulating storage form $25(OH)D_3$ mainly in the liver. $25(OH)D_3$ is further metabolized into the active hormone, $1,25(OH)_2D_3$. Both vitamin D metabolites are inactivated by 24-hydroxylation.

2.1.2 Vitamin D status in humans

Serum 25(OH)D concentration (meaning here the sum of both $25(OH)D_3$ and $25(OH)D_2$, although generally $25(OH)D_3$ is far more abundant in most human individuals) is the established measure for the vitamin D status of human individuals and is used to determine the need of supplementation with vitamin D (7). In accordance, serum 25(OH)D concentration below 50 nM are considered as insufficiency in vitamin D and below 30 nM as vitamin D deficiency according to the suggestions of the Institute of Medicine (IoM) (8).

In contrast, the Endocrine Society suggests that 25(OH)D levels should be at least 75 nM (9). In Finland, the Hospital District of Helsinki and Uusimaa recommends the target level of serum 25(OH)D to be above 50 nM and for good bone health the levels should be even above 80 nM (10). A recent systematic review of 195 vitamin D studies involving more than 168,000 individuals from 44 countries reported that 37% of the participants had 25(OH)D serum concentrations below 50 nM, and only 11.9% were above 75 nM (1). This indicates that vitamin D deficiency or insufficiency is a worldwide problem affecting billions of individuals.

However, there are inter-individual differences in the amount of vitamin D supplementation needed, in order to maintain adequate 25(OH)D levels. Moreover, the recommended doses are under debate. For example, the IoM recommends for healthy adults 15 to 20 μg of daily vitamin D supplementation (8), while the Endocrine Society suggests 50 μg daily (9). Furthermore, one should not forget that human skin has the capacity to generate high amounts of vitamin D_3 in response to sunlight. The production rate of human skin for vitamin D_3 depends on the exposure time to sunlight, skin pigmentation and the intensity of UVB radiation, i.e. time of the day, latitude, and season. In principle, skin is able to produce up to 500 μg vitamin D_3 after a minimal erythema dose of UVB radiation, which can be as short as a 10 min of intensive full body sun exposure of a non-tanned person (4,7). Therefore, humans are able to maintain adequate vitamin D_3 levels through sufficient sun exposure. However, natural UVB exposure is seasonally very limited at higher latitudes (such as in Finland) or due to cultural behavior. In these cases adjusting sufficient intake of vitamin D through diet or supplements is required, in order to maintain healthy vitamin D levels.

Furthermore, an example of additional complexity in evaluating sufficient intake of vitamin D, in order to maintain a health effect of the hormone, is demonstrated by a recent study evaluating vitamin D deficiency among different ethnic groups (11). In this study, 77 or 96% of black adult Americans would be classified as vitamin D-deficient using a threshold 25(OH)D concentration of 50 or 75 nM, respectively. However, the black study participants had a higher bone mineral density, higher calcium levels and only slightly higher PTH levels compared to the white study participants. The study suggests that a polymorphism in the gene coding for the vitamin D-binding protein among African-Americans results in sufficient bioavailability of 25(OH)D despite the lower total concentration of the metabolite.

Obviously, there is great variability between individuals in the effectiveness of vitamin D supplementation. It remains unanswered what is the optimal 25(OH)D level and to what extent it is affected by different factors, such as genetic polymorphisms. Hence, alternative approaches to complement the measurement of the circulating form of 25(OH)D are required, in order to evaluate more precisely the individual benefits and needs of vitamin D. One approach is to measure genomic effects of vitamin D on its target genes. Recently, VDR binding sites were investigated genome-wide in primary $CD4^+$ T cells isolated from nine human individuals (12). Serum 25(OH)D concentration of the individuals varied between 22 and 107 nM. Interestingly, the number of VDR binding sites in T cells varied largely between 200 and more than 7,000, but correlated with the serum 25(OH)D concentration of the individuals. This suggests that the VDR-mediated gene regulation *in vivo* is highly dependent on the vitamin D status of the individual.

A study that analyzed transcriptome-wide mRNA expression profiles in whole blood of more than 200 middle-aged Norwegian women could not identify a single gene being differentially expressed between vitamin D deficient (25(OH)D > 37.5 nM) and sufficient group (25(OH)D > 50 nM) (13). However, when they analyzed differentially expressed gene sets, which have been selected from a large number of public datasets of $1,25(OH)_2D_3$-induced transcriptomes from cell lines, primary cultures, or xenograft mice, they could show that some of these gene sets are differentially expressed between the groups. When analyzing single genes in the most promising gene sets, they found that the genes

thrombomodulin (*THBD*) and cluster of differentiation 14 (*CD14*) were the most significantly contributing to the results of the respective gene sets correlating to vitamin D deficiency. Furthermore, a recent study that monitored 71 pre-diabetic human individuals from the region of Kuopio, Finland, used combined expression changes of the same two genes in peripheral blood mononuclear cells (PBMCs) and adipocytes, in order to evaluate the responsiveness of the individuals to vitamin D_3 supplementation (14). The study found that some of the individuals exhibited a correlation in the changes of their $25(OH)D_3$ levels and their target gene expression levels. The result suggests that the genes *CD14* and *THBD* are suitable biomarkers for representing the transcriptomic response of human tissues to vitamin D_3. Transcriptomic profiling with these genes allowed a categorization of the study participants into responders and non-responders to vitamin D_3.

Taken together, both studies indicate that transcriptomic responses of primary $1,25(OH)_2D_3$ target genes may be suitable for profiling the vitamin D_3 status of human individuals. However, further studies are needed, in order to confirm the classification of human individuals into those that are responding to vitamin D and those that are not. In addition, the most suitable target genes for representing the vitamin D status of human individuals need to be further characterized, in order to successfully evaluate the efficiency of vitamin D supplementation.

2.2 PHYSIOLOGICAL ROLE OF $1,25(OH)_2D_3$

The biological effects of $1,25(OH)_2D_3$ are mediated through binding of the hormone to the transcription factor VDR in the nucleus. VDR binds directly to genomic DNA and preferentially to regulatory region of primary $1,25(OH)_2D_3$ target genes. Subsequently, ligand-activated VDR associates with the basal transcriptional machinery on the gene's transcription start sites (TSSs). This leads to transcriptional activation, which is observed as rapid increase or decrease in the mRNA levels of the gene. The transcriptional regulation by $1,25(OH)_2D_3$ is described in more detail in chapter 2.3.

The best-known physiological role of $1,25(OH)_2D_3$ is the regulation of calcium homeostasis in intestine, bone and kidneys. Severe forms of vitamin D deficiency lead to rickets in children and osteomalacia in adults, which however can be abrogated by vitamin D supplementation (2). $1,25(OH)_2D_3$ enhances intestinal calcium absorption by directly inducing central proteins involved in active intestinal calcium intake (4). Excess calcium is stored in the skeleton, which is the natural calcium reservoir. In response to a decrease in circulating calcium, PTH secretion increases, which leads to the induction of renal *CYP27B1* expression and eventually to an increase in renal $1,25(OH)_2D_3$ production. This results ultimately in the recovery of calcium levels through increased $1,25(OH)_2D_3$-mediated calcium absorption. In situations when dietary calcium is not available in sufficient amounts, increased $1,25(OH)_2D_3$ and PTH levels are able to stimulate bone resorption and to inhibit renal calcium reabsorption, in order to maintain adequate serum calcium levels (2). Vitamin D_3 deficiency reduces the bioavailability of $1,25(OH)_2D_3$, which causes a decrease in intestinal calcium absorption and an increase in PTH levels, which eventually increases bone resorption.

Taken together, a functional vitamin D_3 system is required for maintenance of calcium homeostasis and healthy bones.

2.2.1 $1,25(OH)_2D_3$ and cancer

The biological functions of $1,25(OH)_2D_3$ are not limited to the maintenance of calcium homeostasis. VDR and CYP27B1 are expressed in many human tissues and there is accumulating data of an involvement of $1,25(OH)_2D_3$ in various physiological functions. A prospective 20-year follow-up study of almost 30,000 Swedish women described that their overall mortality rate inversely related to their sun exposure habits, being two-fold higher

among sun avoiders compared with the sun exposure group (15). Although the study did not analyze the causes of death, it suggests that individuals among the sun exposure group had a better vitamin D_3 status and therefore were healthier. Furthermore, several epidemiological studies have shown an association of a low 25(OH)D_3 status, a low vitamin D intake or a reduced sun exposure with various forms of cancer including those of colon, breast and prostate (3,16,17). In addition, molecular and genetic evidence supports the protective role of vitamin D against cancer (3,18). This suggests that vitamin D may inhibit the development or progression of various cancers. This is in accordance with the evidence that solar UVB radiation exposure reduces the risk for several cancers, in particular those of colon and breast (19). In addition, a study analyzing pre-diagnostic 25(OH)D_3 levels among prostate cancer patients observed that low 25(OH)D_3 levels are associated with an enhanced development of metastatic or lethal prostate cancer (20). Although a large number of epidemiological studies and meta-analyzes have shown the beneficial relationship between vitamin D and different cancers, not all studies have found an association with a low vitamin D status and an increased cancer risk (21). In addition, randomized controlled trials on vitamin D supplementation have not yet provided adequate information on the role of vitamin D supplementation in cancer prevention (22). However, epidemiological studies with large cohorts are subjected to number of variations, and even after decades of epidemiological evidence, the protective role of vitamin D against cancer development and progression in population level remains elusive. Therefore, the molecular mechanisms and pathways of vitamin D function need to be further characterized, in order to better understand the protective role of the hormone.

2.2.2 1,25(OH)$_2$D$_3$-mediated cell cycle inhibition

At the cellular level, 1,25(OH)$_2$D$_3$ directly regulates multiple target genes involved in anti-proliferative, pro-differentiating and pro-apoptotic actions in cancer cells. The central mechanism for the anti-proliferative actions of 1,25(OH)$_2$D$_3$ is the induction of cell cycle arrest at the G1 phase of the cell cycle. Cell cycle progression is controlled by cyclins and cyclin-dependent kinases (CDKs) that promote cell cycle phase transitions. In order to activate CDKs, the formation of a cyclin-CDK heterodimer is required. CDK inhibitors (CDKIs) are proteins that prevent the formation of an active cyclin-CDK heterodimeric complex and thereby induce cell cycle arrest (23). 1,25(OH)$_2$D$_3$ directly regulates the expression of the cyclin-dependent kinase inhibitor 1A (*CDKN1A*) gene, which is encoding the CDKI p21 (24,25). The *CDKN1A* gene is discussed in more detailed in chapter 2.4.3.

Another potent CDKI, p27, which is encoded by the cyclin-dependent kinase inhibitor 1B (*CDKN1B*) gene, has elevated levels in 1,25(OH)$_2$D$_3$-mediated G1 cell cycle arrest (26,27). Observations in various cancer cell lines suggest that the detected up-regulation of p27 in response to 1,25(OH)$_2$D$_3$ is mediated through the stabilization of the p27 protein rather than through the induction of *CDKN1B* mRNA. 1,25(OH)$_2$D$_3$ mediates p27 stabilization by a down-regulation of the S-phase kinase-associated protein 2 (encoded by the gene *SKP2)*, which is responsible for the initiation of p27 degradation (28-30). Interestingly, the *SKP2* gene has been identified as a primary VDR target (28). Thus, direct down-regulation of the *SKP2* gene by 1,25(OH)$_2$D$_3$ leads to increase in p27 levels. This suggest that slightly elevated p27 levels, which are often observed together with induced p21 protein concentrations, are secondary effects of 1,25(OH)$_2$D$_3$. Moreover, a study performed in myeloid HL60 and U937 cells demonstrated that 1,25(OH)$_2$D$_3$ down-regulates the expression of microRNA 181 (31). Since microRNA 181 directly suppresses *CDKN1B* gene expression, treatment with 1,25(OH)$_2$D$_3$ leads indirectly to increased *CDKN1B* mRNA levels. In these cell lines, *CDKN1A* has also been characterized as a primary target gene suggesting that 1,25(OH)$_2$D$_3$ regulates cell cycle inhibition both directly and indirectly through *CDKN1A* and *CDKN1B*, respectively. It should be noted that in another study that analyzed both $p21^{-/-}$ and $p27^{-/-}$ mouse embryonic fibroblasts indicated that there are both p27-independent and p27-dependent pathways of 1,25(OH)$_2$D$_3$-mediated cell cycle inhibition (32).

Furthermore, treatment of cells with $1,25(OH)_2D_3$ is associated with a decrease in cyclin D1 and E1 levels, and in CDK2 activity (26,33). However, these responses may be secondary effects of primary $1,25(OH)_2D_3$ target genes, such as *CDKN1A*, which inhibit the activity of cyclins and CDKs. In a study performed on MCF-7 breast cancer cells, $1,25(OH)_2D_3$ suppresses cell proliferation through G1 arrest with temporal elevation of p21 and p27 levels and a decrease in cyclin D1 levels (26). Moreover, a recent study suggests that in this cell line, the growth inhibition by $1,25(OH)_2D_3$ is mainly dependent on insulin-like growth factor binding protein 3 (IGFBP3) and a result of $1,25(OH)_2D_3$-mediated up-regulation of the *IGFBP3* gene (34). IGBFPs are important regulators of the availability of the circulating insulin-like growth factors (IGF) IGF-I and IGF-II, which in turn are important mitogens promoting the growth of normal and malignant cells (35). The genes *IGFBP1*, *IGFBP3* and *IGFBP5* are primary VDR target genes (36). The IGF system is discussed in more detail in chapter 2.4.1. The contradictory observations in MCF-7 cells suggests that the growth inhibition by $1,25(OH)_2D_3$ is not restricted to the regulation of the central cell cycle machinery, but that the hormone simultaneously inhibits cellular growth through a cross-talk with other pathways, including extracellular signals.

Collectively, these observations suggest that $1,25(OH)_2D_3$ inhibits cell cycle progression both directly and indirectly through various target genes that exert control over the cell cycle in many phases by a combination of discrete pathways. Therefore, the molecular basis for the growth inhibition by $1,25(OH)_2D_3$ is exerted through a combination of pathways, which are, in part, tissue-specific.

2.2.3 $1,25(OH)_2D_3$-induced apoptosis and differentiation

An another anti-cancer feature of $1,25(OH)_2D_3$ mediated physiological activity is the induction of apoptosis. $1,25(OH)_2D_3$ has been observed to down-regulate the anti-apoptotic proteins B cell lymphoma 2 (Bcl-2) and Bcl-2 like1 (Bcl-2L1) in breast and prostate cancer cell lines (37,38). Both of these closely related proteins are key factors protecting cells from undergoing apoptosis. Thus down-regulation of these proteins by $1,25(OH)_2D_3$ leads to the induction of apoptosis. Furthermore, artificial overexpression of Bcl-2 in LNCaP prostate cancer cells prevents $1,25(OH)_2D_3$-induced apoptosis but does not affect $1,25(OH)_2D_3$-mediated G1 cell cycle arrest in the same cellular model (37). Accordingly, $1,25(OH)_2D_3$ induces Bcl-2-mediated apoptosis in MCF-7 breast cancer cells (38), where the inhibition of the cell cycle and the modulation of IGF signaling by $1,25(OH)_2D_3$ have already been characterized. As discussed above, the overall effect of $1,25(OH)_2D_3$ on cellular growth is a combination of several signaling pathways.

$1,25(OH)_2D_3$ can also promote the differentiation of some cancer cells, such as the myeloid leukemia lines, U937 and THP-1, into macrophages (24,39). This $1,25(OH)_2D_3$-mediated differentiation changes certain forms of leukemia to a less malignant and more mature phenotype, and is therefore considered as a potential therapeutic and preventive agent for these cancers (40). However, the mechanisms of differentiation include numerous targets and pathways that $1,25(OH)_2D_3$ may control. For example, $1,25(OH)_2D_3$ is associated with the regulation of extracellular signaling through cell surface pathways, such as Wnt/β-catenin, Hedgehog, and Notch, which are involved in cellular differentiation (41). In a study performed in colon cancer cells, $1,25(OH)_2D_3$ induced a differentiated phenotype through the inhibition of the Wnt/β-catenin signaling pathway (42). The Wnt/β-catenin signaling is repressed by $1,25(OH)_2D_3$ via several mechanisms (42,43). First of all, $1,25(OH)_2D_3$ promotes direct VDR-β-catenin interaction, which inhibits transcriptionally active β-catenin. Secondly, $1,25(OH)_2D_3$ enhances nuclear export of β-catenin via increase of E-cadherin. Thirdly, $1,25(OH)_2D_3$ up-regulates the potent Wnt-antagonist gene, Dickkopf WNT Signaling Pathway Inhibitor 1 (*DKK-1*). Generally, the modulation of multiple complex extracellular pathways involved in $1,25(OH)_2D_3$-mediated differentiation is most likely a consequence of the regulation of primary and secondary target genes. Since the process of cellular differentiation is largely dependent on the cell type, the unifying

principles of the general mechanism by which $1,25(OH)_2D_3$ induces differentiation cannot been drawn yet.

2.2.4 Immuno-modulatory actions of $1,25(OH)_2D_3$

The involvement of vitamin D_3 signaling in the regulation of immune function is well established. Several epidemiological studies have reported that a low vitamin D status correlates with the increased risk of developing autoimmune diseases, such as type 1 diabetes, systemic lupus erythematosus, multiple sclerosis, inflammatory bowel disease and rheumatoid arthritis (44). Interestingly, the study previously discussed above, that analyzed differentially expressed gene sets in whole blood mRNA samples between vitamin D deficient and sufficient groups of Norwegian women, found that the majority of differentially expressed gene sets between the groups were related to immune function (13). Those included gene sets involved in innate immunity signaling, cytokine production, chemokine signaling, T cell receptor signaling and Toll-like receptor (TLR) signaling. Most of these are associated with vitamin D deficiency supporting the causal role of vitamin D deficiency in autoimmune diseases.

All central immune cells, such as $CD4^+$ and $CD8^+$ T cells, B cells, neutrophils, and antigen-presenting cells, including monocytes, macrophages and dendritic cells express VDR (45,46). In addition, during $CD4^+$ T cell activation, the low basal expression level of VDR is increased (46). Interestingly, these cells also express the $25(OH)_2D_3$ metabolizing enzyme CYP27B1, which would permit local increases in $1,25(OH)_2D_3$ levels without affecting systemic levels of the hormone. *CYP27B1* expression is induced by various inflammatory signals including interferon-γ (IFN-γ), ligands for the TLR2/1-complex and for TLR4, and viral infections (44). Since $1,25(OH)_2D_3$ target genes include various immune-related genes, locally produced $1,25(OH)_2D_3$ may act in a similar fashion to locally produced cytokines. On the other hand, $1,25(OH)_2D_3$ suppresses the expression of TLR2 and TLR4 (47). TLRs are cell surface receptors expressed in macrophages and dendritic cells and are responsible for the recognition of foreign microbes and the activation of an inflammatory response. As mentioned above, *CYP27B1* expression is induced by TLR2 and TLR4, and therefore the down-regulation of TLRs by $1,25(OH)_2D_3$ suggests that in addition to the inhibition of TLR-mediated bacterial response, CYP27B1-mediated induction of local $1,25(OH)_2D_3$ production may function as feedback regulation for TLR-signaling.

$1,25(OH)_2D_3$ mediates immuno-modulatory functions also through the inhibition of nuclear factor-κB (NF-κB) signaling in various human cells (48,49). NF-κB is a widely expressed transcription factor regulating genes involved in immunity, inflammatory and stress responses. While inactive, NF-κB is kept in the cytosol through the interaction with the protein NF-κB inhibitor (IκBα) that masks the nuclear localization signals of NF-κB. During immune cell activation IκBα is phosphorylated, which leads to subsequent IκBα degradation and thereby making translocation of NF-κB to the nucleus permissible. $1,25(OH)_2D_3$ increases IκBα mRNA and protein levels, which reduces nuclear translocation of NF-κB and thus inhibits its activity (48). In contrast, another study suggested that $1,25(OH)_2D_3$ indirectly inhibits the DNA binding capacity of NF-κB (49). In general, through NF-κB inhibition, $1,25(OH)_2D_3$ is able to suppress the inducibility of genes encoding pro-inflammatory cytokines and chemokines, such as *TNF*, chemokine CXC motif ligand 8 (*CXCL8*) or interleukin 6 (*IL6*), which are regulated by NF-κB.

In addition to general immune suppression through NF-κB inhibition, $1,25(OH)_2D_3$ directly regulates the expression of cytokines. For example, $1,25(OH)_2D_3$ down-regulates the expression of the cytokine genes *IL10*, *IL2* and *IL12B* through primary VDR-mediated regulation (50,51). Analysis in lipopolysaccharide (LPS)-induced human THP-1 monocytes revealed that the *IL10* gene exhibits only short-term primary down-regulation during the first 8 h after $1,25(OH)_2D_3$ treatment. Then its expression returns to basal levels after 24 h (50). This is followed by a delayed secondary effect of a 3-fold up-regulation of the gene after 48 h of ligand treatment. IL10 suppresses the innate immune system through various

mechanisms that include the inhibition of i) the function of macrophages and dendritic cells, ii) monocyte maturation and iii) cytokine expression and secretion (52). Through a transient down-regulation of *IL10* gene expression, $1,25(OH)_2D_3$ allows innate immunity to function before the delayed induction of the cytokine suppresses the innate immune response preventing chronic inflammation (50). Furthermore, in a study using THP-1 monocytes, which were differentiated into macrophages with phorbol 12-myristate 13-acetate (PMA), the *IL1B* gene was characterized as primary $1,25(OH)_2D_3$ target (53). Induction of *IL1B* expression in response to $1,25(OH)_2D_3$ treatment was observed both in non-infected and in *mycobacterium tuberculosis* infected cells. Interestingly, infection enhanced basal VDR binding almost 10-fold to a site located 4.3 kb upstream of the *IL1B* TSS. In response to $1,25(OH)_2D_3$, the chemokine genes *CCL3*, *CCL4*, *CCL8*, *CXCL8* and *TNF* were also induced in both non-infected and infected cells. However, the study did not determine whether those genes are primary VDR targets (53). Nevertheless, secretion of all these $1,25(OH)_2D_3$-induced gene products was observed only in infected cells. This suggests that although $1,25(OH)_2D_3$ promotes the transcriptional up-regulation of cytokines, it does not induce unwanted inflammation in resting cells. In a study performed with primary monocytes derived from healthy controls or from patients with type 1 and type 2 diabetes, treatment with IFN-γ induced the mRNA expression of the cytokines *IL6*, *TNF*, *IL1* and the chemokine *CXCL8* in all three sources of cells (54). The induction was most pronounced in monocytes isolated from type 2 diabetes patients and only in the latter samples $1,25(OH)_2D_3$ could significantly reduce the inducibility of the genes in response to IFN-γ treatment. In contrast, no effects were observed in cells from healthy donors or type 1 diabetes patients. This suggests that $1,25(OH)_2D_3$ is involved in the inhibition of the pro-inflammatory profile observed in type 2 diabetes patients, and may therefore have protective role in controlling type 2 diabetes progression as well.

2.2.5 $1,25(OH)_2D_3$ in adipose tissue

Vitamin D_3 is stored in human adipose tissue. Interestingly, obesity and vitamin D deficiency are known to associate with each other. A large meta-analysis of 21 adult cohorts with 42,024 participants analyzed the causality of the vitamin D status and a high body-mass-index (BMI) (55). By using a Mendelian randomization approach, the study revealed that a high BMI is the reason for a lower systemic vitamin D status. In accordance, individuals who are obese may require a two to three times higher dose of vitamin D_3 supplementation, in order to maintain the same $25(OH)D_3$ levels than individuals with normal weight (9). The observation of a low vitamin D status in obesity suggests that vitamin D deficiency may have a role in the adverse health effects originally associated with obesity. However, which are underlying mechanisms that lead to the suppression of vitamin D levels in individuals who are obese, is still under debate. It is suggested that obesity reduces the bioavailability of vitamin D_3, since orally supplied vitamin D is sequestrated in visceral fat, while subcutaneous fat stores vitamin D_3 after its synthesis in the skin (56). Another study suggests that large volumetric dilution in obese individuals explains the low vitamin D availability (57).

Human adipose tissue is not only a storage site for vitamin D_3 but adipose cells express VDR and are subject to $1,25(OH)_2D_3$-dependent gene regulation. A microarray study performed with adipocytes derived from subcutaneous fat revealed that 237 genes respond to $1,25(OH)_2D_3$. These genes were largely related to inflammation and oxidative stress (58). However, the lack of genome-wide VDR binding data in adipocytes does not allow an evaluation how many of the responding genes may be primary $1,25(OH)_2D_3$ targets. Furthermore, microarray studies that used human Simpson-Golabi-Behmel syndrome (SGBS) adipocytes, which had been treated with medium derived from PMA-differentiated U937 macrophages, indicated an impact of macrophage signaling on the vitamin D_3 system in adipocytes (59). This interesting approach revealed a high inducibility of the *CYP27B1* gene (more than 10-fold after 4 h of treatment and even 82-fold after 24 h) in response to

macrophage-conditioned medium. Although the factors which up-regulate *CYP27B1* expression are unknown, the observation is similar to that in monocytes/macrophages, where *CYP27B1* expression is strongly up-regulated in response to various inflammatory signals (44). The increase in *CYP27B1* mRNA expression suggests that during infection, adipose tissue functions as a site for local $1,25(OH)_2D_3$ production. Interestingly, macrophage-conditioned medium also increases VDR protein expression after 24 h of treatment (59). This suggests that macrophage signaling promotes intracellular $1,25(OH)_2D_3$ regulation, and not only the production of the hormone.

$1,25(OH)_2D_3$ regulates the expression of several cytokines in adipocytes. In a study that used primary subcutaneous adipose tissue cells and adipocytes differentiated from bone marrow-derived human mesenchymal stromal cells, co-treatment with $1,25(OH)_2D_3$ and LPS reduced the ability of LPS to induce IL6 secretion (60). In addition, pre-treatment with $1,25(OH)_2D_3$ for 24 h sequestered LPS-mediated inducibility of mRNA and protein secretion of IL6. It was shown that in both cell types $1,25(OH)_2D_3$ inhibited NF-κB translocation to the nucleus by increasing IκBα availability. Thus, pre-treatment with $1,25(OH)_2D_3$ blocks NF-κB inducibility and prevents LPS to induce IL6. Another study reported that in pre-adipocytes derived from subcutaneous adipose tissue, $1,25(OH)_2D_3$ reduced the basal secretion of CCL2, CXCL8 and IL6 (61). Similarly, as in the previous study, these reductions in cytokine expression were associated with $1,25(OH)_2D_3$-mediated induction of IκBα. Interestingly, basal secretion of CCL2, CXCL8 and IL6 was strongly reduced when the pre-adipocytes were differentiated into mature adipocytes. In a study performed with human SGBS pre-adipocytes, the expression levels of all 48 human NRs were analyzed during the differentiation process from pre-adipocytes to adipocytes (62). It was found that 15 of the 30 expressed NRs, including VDR, are significantly down-regulated during differentiation, while only six NR genes had increased mRNA expression. This suggests that $1,25(OH)_2D_3$ may have a more profound effect in pre-adipocytes compared to mature adipocytes.

In summary, adipocytes exhibit active $1,25(OH)_2D_3$ signaling and have the potential to synthesize $1,25(OH)_2D_3$ locally. The observed reduction in inflammation via a down-regulation of cytokines resembles that of immune cells. However, due to the lack of genome-wide VDR binding data, little is known about the global primary response to $1,25(OH)_2D_3$ in adipocytes.

2.3 VITAMIN D RECEPTOR

$1,25(OH)_2D_3$ mediates all of its biologically relevant functions through the activation of the transcription factor VDR. VDR is a member of NR superfamily that consists of 48 ligand-activated, DNA binding receptors, which are important regulators of gene expression (63). Regulation of gene expression by NRs mediates immediate transcriptional response of their ligands, such as dietary lipids, vitamin A and D, steroid and thyroid hormones. Therefore, NRs are important ligand-inducible switches during cellular metabolism, growth and differentiation. Since $1,25(OH)_2D_3$ is the only natural high affinity ligand for VDR, the physiological consequence of $1,25(OH)_2D_3$ signaling is mostly, if not solely, the outcome of VDR action. Moreover, VDR is widely expressed, and therefore most human tissues are responsive to $1,25(OH)_2D_3$ (64).

Like most other NRs, the VDR protein is composed of a non-conserved amino-terminal domain, followed by a highly conserved DNA-binding domain (DBD), a non-conserved hinge domain and a structurally conserved carboxy-terminal ligand-binding domain (LBD) (65). The DBD contains two tandem zinc finger motifs that mediate sequence-specific DNA binding. The DBD and the LBD are connected by the hinge region, whose flexibility allows the DBD to efficiently bind DNA in various receptor conformations. The VDR hinge region also harbors a nuclear localization signal. In addition, the hinge region stabilizes the DBD-DNA-complex and is therefore required for efficient DNA binding of the receptor (66). The

LBD contains a ligand-binding pocket (LBP), which allows specific ligand recognition. The inner surface of the LBP is formed of some 40 non-polar amino acid residues and three pairs of polar anchoring points that explain the high specificity of LBP toward its respective ligand (63). However, the volume of the LBP varies significantly between NRs being between 400 and 1400 $Å^3$.

In addition to ligand-binding properties, the LBD mediates associations with other transcription factors and co-regulatory proteins (67). For more details see the following chapter.

2.3.1 Mechanism of $1,25(OH)_2D_3$ target gene regulation by VDR

$1,25(OH)_2D_3$ is a small lipophilic molecule that can directly activate VDR-mediated transcription in the nucleus. Gene regulation by systemic, extracellular $1,25(OH)_2D_3$ does not require additional signal transduction steps. When $1,25(OH)_2D_3$ docks into VDR's LBP, a conformational change on the surface of the LBD occurs, which in turn, alters the protein-protein interaction profile of the receptor (63). Thus, $1,25(OH)_2D_3$ triggers the interaction of DNA-bound VDR with other transcription factors and with the basal transcriptional machinery. This allows the receptor to directly modulate the expression of its target genes. In order to form a stable VDR-DNA complex, VDR requires complex formation with another DNA-binding partner protein. Ligand-activated VDR interacts preferentially with the retinoid X receptor (RXR), i.e. it forms a heterodimer. The DBDs of VDR and RXR both recognize the hexameric DNA consensus sequence RGKTSA (R = A or G, K = G or T, S = C or G) and due to steric constrains of the VDR-RXR complex, the optimal binding motif is formed by a direct repeat of two core binding sequences spaced by three nucleotides (DR3) (68,69). However, genome-wide VDR binding site analyses have indicated that only the minority of all VDR loci contains the classical DR3-type binding motif. This is further discussed in the next chapter.

Even in the absence of ligand, VDR is able to bind to DNA, although in this case the VDR pool is spread between cytoplasm and nucleus. $1,25(OH)_2D_3$ stimulation promotes greater nuclear localization of the receptor, its dimerization with RXR and subsequent DNA binding (70). Similarly, analyses of genome-wide VDR binding sites have shown that the number of occupied VDR binding sites in the human genome increases in response to VDR ligand stimulation (71). When VDR is bound to DNA in the absence of ligand, the receptor associates with co-repressors, such as NCoR, SMRT and Cops2 (also known as Alien) (72,73). Co-repressors mediate transcriptional repression through a direct inhibition of the transcription machinery and via the recruitment of repressing chromatin modifiers, such as histone deacetylases (HDACs). During ligand-induced VDR activation the conformational change on the VDR-LBD surface causes the release of co-repressors and HDACs and is followed by the recruitment of co-activators. A large number of co-activators, including the multi-subunit mediator complex, form a bridge between the VDR and the TSS regions of its target genes. This enables the interaction of VDR with the basal transcriptional machinery containing RNA polymerase II, leading to the initiation of gene transcription (74,75).

Although the initiation of mRNA synthesis by $1,25(OH)_2D_3$ is caused through the interaction of VDR with the transcriptional machinery, the process is not always continuous, since cyclical accumulation of some VDR target gene mRNA levels has been observed. Furthermore, it has been shown that cyclical induction of the VDR target gene *CDKN1A* mRNA, in response to $1,25(OH)_2D_3$, results from the cyclical association of VDR with binding sites nearby the *CDKN1A* gene (76). In addition, expression of the estrogen receptor target gene trefoil factor-1 (77) and that of the VDR-induced *CYP24A1* gene (78,79) are the result of similar cyclical association of the receptor, RNA polymerase II and co-factors with the respective gene promoters.

Taken together, transcriptional cycling is a consequence of a dynamic oscillation of chromatin activation and repression phases (80). Compared to a stable formation of VDR-

RNA polymerase II complexes, a dynamic regulation of transcription enhances the control over the transcription process mediated by NRs.

2.3.2 Genome-wide VDR locations

Chromatin immunoprecipitation (ChIP) is an experimental technique that is used to quantify interactions between specific proteins and genomic DNA. It is often used to monitor the binding of transcription factors to their genomic targets or to detect the presence of specific histone modifications. ChIP combined with massive parallel DNA sequencing (ChIP-seq) provides a genome-wide view of transcription factor binding. During this thesis project, VDR ChIP-seq data from undifferentiated THP-1 monocytic cells (81), LPS-differentiated macrophage-like THP-1 cells (71), immortalized lymphoblastoid cell lines GM10855 and GM10861 (82), LX2 hepatic stellate cells (83) and LS180 colon cancer cells (84) have been used. Since in the original studies, different analysis software and thresholds for peak determination were applied, the number of peaks (that equate to VDR binding sites) was not fully comparable between the datasets. Therefore a harmonized re-analysis of the original data by using standardized protocols was recently performed in order to allow cross data set comparisons (71).

The total number of VDR binding locations increased in all six cellular models after the cells were treated with VDR ligand. The increase in peak number was greatest in LS180 cells, where VDR bound only to 165 genomic regions in the absence of ligand, while after 3 h of $1,25(OH)_2D_3$ treatment almost 3,800 VDR binding sites were occupied. In contrast, in LX2 cells 20 h treatment with VDR ligand kept the number of VDR peaks in the order of 1,500. Highest total number of VDR peaks was observed in the lymphoblastoid cell lines GM10855 and GM10861, with more than 6,000 and 12,000 peaks after 36 h of $1,25(OH)_2D_3$ treatment, respectively. Similar to the increase in VDR binding sites in response to ligand treatment, the ChIP-seq study that used primary T cells isolated from nine human individuals (12) showed that the number of VDR peaks, which varied between 200 and 7,000, correlates with the serum 25(OH)D concentration of the individuals. However, the raw data for this study is not available for further analysis and therefore the number of peaks is not directly comparable with that of the harmonized analysis (71).

In total, the six ChIP-seq datasets revealed that there are more than 20,000 unique VDR binding sites. The actual number depends slightly on the maximum allowed distance between the peak summits. Interestingly, when allowing that the peak summits may differ in maximum by 250 bp, almost 70% of the peaks are cell type specific, i.e. they are found uniquely in one cell line tested. Importantly, under this condition, only 55 VDR binding loci are conserved in all six cell lines suggesting that VDR signaling and the number of genomic binding sites is very cell type dependent.

A screening for transcription factor binding motif below the summits of VDR peaks identified DR3-type sequences as the dominant VDR binding site in all six cell types (71). However, only some 2,500 of the more than 20,000 VDR binding sites carry this classical DR3-type motif, but the DR3 occurrence rate is largely dependent on the cell type. Nevertheless, the prevalence of DR3-type sequences correlates with the size (fold enrichment value) of the VDR peak. Prominent VDR peaks represent, in general, strong VDR binding and good quality of the ChIP signal. When the VDR peaks were sorted by their fold enrichment value, the DR3 rate of occurrence in the group of weakest VDR binding sites was below 20%, while in the group of the most prominent peaks, the DR3 rate of manifestation ranged between 70 and 90%. When all VDR sites are taken into account, the DR3 incidence rate in ligand-treated cells was higher than in unstimulated samples. This suggests that many of the non-DR3-type VDR binding sites in unstimulated cells may function as temporary nuclear storage places for VDR, from where the receptor is shifted to the active DR3-type locations during ligand-activation. However, the existence of prominent, non-DR3-type VDR sites in all cell types indicates that these types of sites can be biologically active and participate in $1,25(OH)_2D_3$-mediated gene regulation. The nature

of these sites is unknown. However, it has been suggested that, at these sites, VDR forms a heterodimer with a presently undefined DNA binding partner or may complex with other DNA binding proteins, such as pioneer factors, without direct DNA binding (74).

2.3.3 Chromatin remodeling in relation to VDR-mediated gene regulation

In order to fit into the nucleus, genomic DNA is tightly packed around histone octamers forming nucleosomes (85). The nucleosome fiber is further condensed into higher order chromatin structures. This highly condensed chromatin is transcriptionally inactive and not accessible to most transcription factors. VDR belongs to the latter and has to overcome the repressive nature of condensed chromatin, in order to access its binding loci. As mentioned earlier, in the absence of $1,25(OH)_2D_3$ VDR associates with HDACs. This generates and promotes condensed chromatin structures by deacetylating histones, which prevents transcriptional activation (73). In contrast, some of co-activators that interact with VDR after ligand activation possess histone acetyltransferase (HAT) activity. This induces histone acetylation, which in turn opens condensed chromatin, in order to make it accessible for other transcription factors (85). Opening of compacted chromatin is a prerequisite for transcription factors to activate transcription. Via complex formation with chromatin modifiers ligand-induced VDR mediates local chromatin relaxation and increases the accessibility of other factors involved in transcription. Therefore, $1,25(OH)_2D_3$-induced chromatin opening is one hallmark of a prominent VDR binding site.

Genome-wide rates of open chromatin can be analyzed by using formaldehyde-assisted isolation of regulatory elements (FAIRE) combined with massive parallel sequencing (FAIRE-seq). A time course FAIRE-seq analysis of $1,25(OH)_2D_3$-mediated chromatin opening in THP-1 monocytes demonstrated that some 87% of the 1,000 VDR binding sites in these cells are located on open chromatin (86). Interestingly, at 165 VDR binding sites $1,25(OH)_2D_3$ induces a strong increase of chromatin accessibility within 2 h after ligand treatment, 66% of which contain a DR3-type sequence. This is more than double than the average DR3 occurrence rate in this cellular model. In contrast, from the 500 VDR binding sites, whose chromatin accessibility was unchanged by $1,25(OH)_2D_3$ treatment, only less than 20% have a DR3-type sequence residing below the VDR peak summit.

Taken together, genome-wide data of dynamic ligand-mediated chromatin opening emphasize the dominant role of DR3-type motifs as the preferred site for VDR binding. A DR3-type site, together with ligand-inducible chromatin opening, is therefore a good indicator for the regulation of a primary VDR target gene in the relative vicinity of the site.

2.4 CENTRAL $1,25(OH)_2D_3$ TARGET GENES

2.4.1 The *IGFBP3* gene

The *IGFBP3* gene, a member of *IGFBP* gene family, is located on chromosome 7 next to the *IGFBP1* gene and encodes a secreted protein of 291 amino acids in size. There are six members in the IGFBP protein family that bind IGFs with high affinity, IGFBP1 through IGFBP6. The IGFBP3 protein is the most abundant member of the protein family (87). IGFBPs are important modulators of the IGF system, which consists of IGF-I and IGF-II and their cell surface receptors IGF-IR, IGF-IIR, as well as the insulin receptor (88). IGF-I and -II are important mitogens promoting cellular growth and metabolism of normal and malignant cells. IGFs are produced mainly by the liver in response to growth hormone and mediate their mitogenic effects primarily through activating IGF-IR (35). Normally, IGFs are bound almost exclusively to IGFBPs, and since IGFBP3 is the most abundant IGFBP in circulation, it represents the major IGF binding capacity in serum (35,87). Additionally, the affinity of IGFBP3 for IGFs is higher than their affinity to the membrane bound receptors. Therefore, IGFBP3 can regulate the availability of IGFs and either inhibit or enhance their

action (89). In addition, IGFBP3 proteins exhibit a tissue-specific expression pattern and are therefore able to regulate IGF-mediated growth control locally.

Due to the central role of IGFBP3 in the regulation of IGF-induced cellular growth, the transcriptional regulation of the *IGFBP3* gene, such as its up-regulation by $1,25(OH)_2D_3$ or its synthetic analogs, controls also the activity of IGFs. This explains the anti-cancer effects of IGFBP3 (34,90). Furthermore, IGFBP3 has been shown to regulate cellular growth also in an IGF-independent fashion. IGFBP3 was suggested to translocate to the nucleus and directly regulate target gene expression by forming a heterodimer with RXR (91). Moreover, when not bound with IGFs, IGFBP3 can activate cell surface receptors, such as transforming growth factor-β (TGF-β) receptor, or induce caspase-mediated apoptosis (35).

The important role of IGFBP3 in $1,25(OH)_2D_3$-mediated regulation of cellular growth is well established. Growth inhibition of MCF-7 and Hs578T human breast cancer cells mediated by $1,25(OH)_2D_3$ analogs is associated with increased IGFBP3 production (90). In addition, in a study performed in LNCaP prostate cancer cells, $1,25(OH)_2D_3$-mediated growth inhibition showed to be dependent on IGFBP3 (92). The inhibition of cellular growth mediated by the hormone was abolished when $1,25(OH)_2D_3$-induced *IGFBP3* expression was withdrawn using anti-sense oligonucleotides against *IGFBP3*. This $1,25(OH)_2D_3$/IGFBP3-mediated growth inhibition was further associated with increased amounts of p21 protein, which had been induced by IGFBP3. Since the gene *CDKN1A*, encoding p21, has been also characterized as primary $1,25(OH)_2D_3$ target gene (25) suggesting that $1,25(OH)_2D_3$ may target the gene both directly as a result of hormone action and indirectly via IGFBP3 mediated events.

In a recent study, MCF-7 breast cancer cells were used along with MCF-7/VD^R cells, which are resistant to both the growth inhibitory and the apoptosis inducing signals of $1,25(OH)_2D_3$ (34). The use of these cellular models demonstrated that the impaired secretion of IGFBP3 protein was associated with the inability of $1,25(OH)_2D_3$ to inhibit the growth of vitamin D resistant MCF-7/VD^R cells. The study provided additional evidence that the *IGFBP3* gene has a central role in $1,25(OH)_2D_3$-mediated growth inhibition in human breast cancer cells. Furthermore, the regulation of the *IGFBP3* gene by $1,25(OH)_2D_3$ has been studied in the prostate cancer cell lines LNCaP and PC-3 and in the osteosarcoma cell line SaOS-2 (36,93). In these studies, two functional VDR binding regions were shown to mediate the primary response of the *IGFBP3* gene to $1,25(OH)_2D_3$.

In summary, all these observations support the view that the primary $1,25(OH)_2D_3$ target gene, *IGFBP3*, is an important regulator of cellular growth and apoptosis.

2.4.2 The G0/G1 switch 2 *(G0S2)* gene

The *G0S2* gene is located on chromosome 1 and encodes a small 103 amino acid long protein. Initially, the protein was associated with the transition of the cell cycle of cultured mononuclear cells from G0 to G1 phase *(94)*. However, since then a variety of functions for G0S2 have been described, such as the ability to reduce the growth of leukemia cells (95). The involvement of G0S2 in proliferation, carcinogenesis and metabolism makes it a multi-functional protein (96). The *G0S2* gene exists only in vertebrates but is highly conserved between species, such as a 78% homology between human and mouse. In the cytoplasm G0S2 is anchored to the membranes of the endoplasmic reticulum and mitochondria (97,98).

The $1,25(OH)_2D_3$-mediated regulation of *G0S2* was long time overlooked, but in microarray expression studies the gene was found to be $1,25(OH)_2D_3$ responsive in breast, colon and squamous cell carcinoma cell lines (99). In addition, in a study that used two different prostate-derived cell lines, the *G0S2* gene was up-regulated in RWPE-1 cells that are responsive to anti-proliferative actions of $1,25(OH)_2D_3$, whereas it was down-regulated in PC-3 cancer cells that are insensitive to $1,25(OH)_2D_3$-mediated growth inhibition (100). The *G0S2* gene is also regulated by peroxisome proliferator-activated receptors (PPARs), and its mRNA expression is induced during differentiation of both human SGBS and

mouse 3T3-L1 pre-adipocytes (98). Interestingly, increased *G0S2* expression is observed during growth arrest of 3T3-L1 cells, which is an essential step in their initiation of differentiation into adipocytes. These observations suggest that G0S2 is associated with adipogenesis via its involvement in growth arrest.

In hematopoietic stem cells G0S2 inhibits proliferation and promotes them into a quiescent state through a direct interaction with nucleolin (97). Nucleolin is a multi-functional protein that promotes cellular growth by regulating ribosomal RNA and DNA metabolism in the nucleus. Increased cellular levels of G0S2 reduce nucleolin availability in the nucleus by direct sequestration in the cytosol, which eventually leads to the inhibition of stem cell proliferation. The role of nucleolin in promoting stem cell proliferation is supported by observations that show that nucleolin expression is increased in rapidly dividing normal and cancer cells (101).

Suppressed *G0S2* expression, caused by hypermethylation of its gene promoter, is observed in cancer cell lines and tumor samples (96). This suggests that functional G0S2 protein has a role in the prevention of carcinogenesis. Moreover, the protein may act as a tumor suppressor, since methylation of the *G0S2* promoter leads to malignant transformation. Moreover, in a recent study the suppression of the *G0S2* gene in K562 human myeloid leukemia cells was associated with methylation of its proximal promoter and exon 1 (95). When *G0S2* expression was restored either by demethylation or by gene expression brought by viral transduction, cellular proliferation was reduced. Furthermore, in a nude mouse xenograft model for chronic myeloid leukemia tumor growth could be significantly inhibited by *G0S2* overexpression. In summary, all these findings support the idea that the *G0S2* gene is a tumor suppressor in hematopoietic cells.

The ability of G0S2 to inhibit hematopoietic stem cell proliferation suggests that sufficiently expressed *G0S2* may participate both in inhibiting carcinogenesis and in suppressing tumor growth in the whole hematopoietic system. Although G0S2 may have largely tissue-specific functions, its significant role as a tumor suppressor in human leukemia cells offers a great therapeutic potential in the development of new leukemia therapeutics. Since the gene is suppressed in leukemic cells, especially the mechanisms for recovering its functional expression should be focused upon.

2.4.3 The *CDKN1A* gene

The *CDKN1A* gene is located on chromosome 6 and encodes the well-known CDKI protein p21. The gene was identified originally as a mediator for the tumor suppressor protein p53-induced cell cycle arrest in response to DNA damage (102). When induced by p53, p21 promotes cell cycle arrest by directly interacting with both cyclins and CDKs. This efficiently prevents the formation of functional cyclin-CDK dimers and leads to a G1 phase cell cycle block (23). In addition, small interfering RNA (siRNA) silencing of *CDKN1A* gene expression in LNCaP prostate cancer cells abolished growth inhibition mediated by $1,25(OH)_2D_3$ (103). This suggest that, at least in this cell line, p21 is responsible for mediating the majority of the anti-proliferative actions of $1,25(OH)_2D_3$. Interestingly, lower intracellular p21 levels are suggested to promote cyclin-CDK assembly and continuation of the cell cycle, since normal physiological levels of p21 have been shown to be required for a fully functional cyclin-CDK system (104). Thus, p21 has a dual role in cell cycle control: normal levels are required for cell cycle progression, whilst elevated levels of the protein lead to cell cycle arrest. Independent of the cyclin-CDK system, p21 inhibits DNA synthesis during the S phase of the cell cycle through PCNA (proliferating cell nuclear antigen, a processivity factor for DNA polymerase δ), which controls the rate of DNA synthesis during DNA replication (105). Through a direct interaction with PCNA, p21 blocks other DNA replication factors from binding to PCNA, and this results in the inhibition of DNA replication. Interestingly, Myc protein, encoded by the gene v-myc avian myelocytomatosis viral oncogene homolog (*MYC*), interacts with the same domain of p21 as PCNA (106). Therefore, Myc is able to disturb the inhibition of DNA synthesis mediated by p21.

In addition to its fundamental role in cell cycle regulation, p21 is associated with apoptosis and differentiation. The p53-mediated induction of p21 leads to cell cycle arrest, which also protects cells from direct p53-mediated apoptosis. In addition, in a study performed in lung carcinoma cells, p53-induced p21 inhibited the function of caspase-2, which, in turn, repressed apoptosis initiation (107). Moreover, in hepatoma cells committing caspase-mediated apoptosis p21 protein is cleaved by activated caspase-3, while in cells overexpressing p21 caspase-3-mediated apoptosis is suppressed (108). The observations that p21 protects against apoptosis and promotes cell cycle arrest suggest that it is involved in the decision, whether cells commit apoptosis or enter cell cycle arrest. Since cell cycle arrest is required for terminal differentiation, p21 is able to induce differentiation of both malignant and non-malignant cells (23). For example, p21 facilitates differentiation of U937 human myelomonocytic cells (24). Although p21 has an important role in induced differentiation, in p21 knockout mice, normal differentiation of epidermal cells has been observed. This suggests that under normal physiological conditions p21 is not essential for the differentiation process (109).

Repression of the *CDKN1A* gene by mutations is very rare in human cancers. However, *CDKN1A* deficient mice are more prone to develop cancers upon exposure to γ-irradiation. Moreover, *CDKN1A* null mice show an increased trend of tumor metastasis, suggesting a role of *CDKN1A* in cancer prevention (110). Elevated cytoplasmic expression levels of *CDKN1A* have been associated with the progression of various cancers (111) indicating its role in carcinogenesis. Furthermore, oncogene proteins, such as HER-2/neu, are able to retain p21 in the cytoplasm and thereby prevent p21-induced growth arrest (112). Therefore, altering the subcellular location of p21 is one important aspect when evaluating the therapeutic potential of p21.

CDKN1A was characterized first in U937 cells as up-regulated $1,25(OH)_2D_3$ target gene being regulated via a VDR binding site close its TSS (24). In MCF-7 cells the screening of 7 kb of the *CDKN1A* promoter revealed three additional VDR binding sites (76). However, the VDR binding site described in U937 cells was not confirmed in MCF-7 cells, suggesting a cell-specific regulation of the gene. In addition, the gene is up-regulated indirectly by $1,25(OH)_2D_3$ via IGFBP3 or TGF-β dependent mechanisms (26,92). Therefore, the transcriptional regulation of the *CDKN1A* gene and the functionality of its protein product p21 in growth inhibition should be evaluated in a tissue- and cell-specific manner.

2.4.4 The *MYC* gene

The proto-oncogene *MYC* is located on chromosome 8 and encodes the transcription factor Myc, which is a critical regulator of cellular growth. The gene is one of the most studied targets for cancer therapy, since it is dys-regulated in the majority of cancers and its inhibition is associated with reduced cellular growth. The *MYC* gene is ubiquitously expressed and Myc protein participates in normal gene regulation, primarily as a heterodimer with Myc-associated factor-X (Max) (113). Myc is an important regulator of gene expression and has global effects on the human transcriptome. It has been estimated that Myc regulates some 15% of all human genes (114,115). The observed proportion of the genes involving Myc in their regulation is even higher among actively transcribed genes (116). Moreover, ChIP-seq analyses have shown that Myc has several thousand genomic binding sites, not all of which contain the traditional binding motif (117,118). The evaluation of genomic Myc binding sites in the context of microarrays showed that almost 80% of the Myc-dependent genes had an active Myc binding site within 1 kb of their TSS region (117). This suggests that most of the Myc target genes are under the primary control of the protein. In addition, Myc protein controls transcriptional elongation by pausing RNA polymerase II (116). Promoter-proximal pausing (the regulation of transcription during the elongation phase of transcription), is a widespread regulatory mechanism in higher eukaryotes. Furthermore, Myc has been shown to modulate mRNA cap methylation and DNA replication (114). Finally, DNA-bound Myc without transcriptional activity has

shown to initiate DNA replication (119) and overexpression of *MYC* leads to increase in replication origin activity.

Dys-regulation or increased expression of the *MYC* gene is observed in the majority of human cancer types. The gene is also the most amplified oncogene in human cancers. In an analysis of more than 3,000 tumor copy number profiles, from 26 cancer types, *MYC* gene chromosomal amplification was found to be the most frequent event, affecting 14% of all samples (120). The inhibition of Myc protein expression reduces the growth of cultured cells. Moreover, in a pre-clinical mice model for lung tumor, the suppression of Myc function resulted in rapid regression of the tumor with increased apoptosis (121). However, in continuously proliferating tissues the systemic inhibition of *MYC* gene expression resulted in side effects: mice showed a reduction in skin and hair growth and a reduced cell proliferation in testis and intestine, although no apoptosis was observed. This outcome is however expected, since Myc has an essential role in the proliferation of all normal cells. Nevertheless, one week after Myc inhibition was stopped, all side effects were reversed and the mice showed a normal phenotype. Therefore, down-regulation of the *MYC* expression is of great interest in the development of new cancer therapies.

It has been already more than 30 years since the *MYC* gene was reported to be a down-regulated $1,25(OH)_2D_3$ target (122). In the intervening years, *MYC* gene regulation by $1,25(OH)_2D_3$ has been identified in several cellular models, such as in RWPE-1 prostate cells, where *MYC* is a rapidly down-regulated primary $1,25(OH)_2D_3$ target (123). Therefore, the reported effects of $1,25(OH)_2D_3$ in mediating growth inhibition or to induce apoptosis are most likely reflecting the cellular responses evoked by the down-regulation of the *MYC* gene, to some extent. However, it should be noted that in cancers, where *MYC* gene amplification is common, not all distal regulatory elements of the gene may be copied with the original gene and $1,25(OH)_2D_3$ may not have the same effect on the regulation of *MYC*.

In summary, Myc directly modulates a large number of genes and pathways, thus even small changes in *MYC* gene expression may have a significant global impact on cellular growth. In addition, the gene is associated strongly with the majority of human cancers and therefore the mechanisms behind its primary regulation are of great interest.

2.4.5 The chemokine cluster

Orchestrated cell recruitment and positioning is a central event in immune response. The most important coordinators of leukocyte trafficking are chemokines, which are small chemoattractant cytokines. The first chemokine, which was identified more than 25 years ago, is the potent neutrophil activator CXCL8, also known as IL8 (124). Since then, approximately 50 human chemokines and more than 20 chemokine receptors have been characterized. The chemokine group is divided into four families, C, CC, CXC, and CX3C, based on their cysteine motifs (125). In the CC chemokine family, the first two cysteine residues are next to each other, in the CXC chemokines the cysteine residues are separated by one amino acid, while within the only characterized member of CX3C chemokines, CX3CL1, the cysteine residues are separated by three amino acids. In the group of C chemokines, there is only one cysteine residue. Besides these structural criteria, chemokines can be categorized also into functional groups, such as inflammatory, homeostatic, dual-function and platelet chemokines, but this classification is not comprehensive (125,126).

Inflammatory chemokines are up-regulated in response to inflammation and act to direct cellular chemotaxis towards the site of inflammation. Homeostatic chemokines, on the other hand, are constantly expressed and participate in the regular trafficking as well as localization of lymphocytes and dendritic cells throughout the body (126). In contrast to inflammatory chemokines, homeostatic chemokines are relatively conserved between species (125). The group of platelet chemokines consists of important regulators for platelet development and maturation. They are associated with platelet activation, vascular repair and angiogenesis and are stored at high concentrations in platelets (127).

Vertebrates exhibit significant differences in the total number of chemokines (128). Humans and mice display many differences in their inflammatory chemokine profile. For example, the *CXCL8* gene exists only in humans. This suggests that mammalian inflammatory chemokine genes are the result of the rapid and divergent evolution. Moreover, many chemokine genes are located in chemokine clusters spread throughout the human genome. The CC chemokine cluster on chromosome 17 comprises 12 genes, while the CXCL chemokine gene cluster on chromosome 4, spanning over 350 kb, contains the nine genes *CXCL1* to *CXCL8* and *CXCL4.1*. The members of the latter chemokine cluster are classified as inflammatory chemokines with the exception of the platelet chemokine *CXCL4* and its variant *CXCL4.1* (125). In addition, all seven inflammatory chemokines carry an angiogenic Glu-Leu-Arg (ELR) motif prior the first cysteine motif in their protein sequence (129). Chemokines with an ERL motif are the main chemoattractants for neutrophils and are able to mediate angiogenesis (129,130). Interestingly, the ELR motif is not found outside of the CXCL cluster and therefore the seven angiogenic chemokine genes of the CXCL cluster form a unique set of human neutrophil chemoattractants that are able to coordinate the connection between inflammation and angiogenesis. Although the main function of the inflammatory chemokines of the CXCL cluster is neutrophil chemotaxis in inflammation, angiogenic CXC chemokines are also able to promote cancer progression (131). In addition, elevated expression of angiogenic chemokines has been associated with angiogenesis, tumor growth and increased metastasis.

Recruitment of neutrophils is one the first immune responses during infection. Therefore, the release of chemokines from the CXCL cluster is the first signal involved in acute inflammation. The CXCL8 chemokine is a prototypical member of the CXC chemokine family and is the most potent chemokine mediating neutrophil chemotaxis (130). CXCL8, and its relative CXCL6, bind with high affinity to the G-protein-coupled receptors CXCR1 and CXCR2, which are found on the surface of neutrophils. In contrast, the other CXCL cluster chemokines mediate their actions solely through the CXCR2 receptor (130,132). The neutrophil recruitment activity of chemokines is regulated largely by post-translational modifications (130). In addition, dimerization of CXCL8 reduces its receptor affinity and neutrophil recruitment potential (132). However, since inflammatory chemokines are not stored intracellulary, the transcriptional regulation of the *CXCL* cluster genes is also important for CXC chemokine function. For example, various inflammatory signals are able to induce *CXCL8* transcription via NF-κB-mediated primary regulation of the gene (133).

In a study that used monocytes from type 2 diabetes patients, cells having a pro-inflammatory profile and high *CXCL8* expression levels, co-treatment with $1,25(OH)_2D_3$ inhibited IFN-γ-mediated induction of the *CXCL8* gene (54). In contrast, in a recent study performed in PMA-differentiated THP-1 macrophages, $1,25(OH)_2D_3$ induced *CXCL8* expression more than 10-fold after 24 h treatment (53). Furthermore, when cells were infected by *mycobacterium tuberculosis*, which resulted in high *CXCL8* induction, $1,25(OH)_2D_3$ could promote the transcription rate of *CXCL8* even further. Consistently with this, $1,25(OH)_2D_3$ treatment resulted in increased secretion of CXCL8 protein in infected cells. However, $1,25(OH)_2D_3$ did not increase the secretion of the CXCL8 protein in absence of mycobacterium infection. This suggests that, although $1,25(OH)_2D_3$ promotes the transcriptional regulation of the gene in resting macrophages, it is not resulting in unwanted inflammation. However, neither of these studies investigated whether *CXCL8* is primary target of $1,25(OH)_2D_3$.

2.4.6 The *ASAP2* gene

The ArfGAP with SH3 domain, ankyrin repeat and PH domain 2 (*ASAP2*) gene encodes a large 1,006 amino acids multi-domain protein that is expressed in multiple tissues. The Asap2 protein is composed of an N-terminal α-helical region with a coiled-coil motif, followed by a pleckstrin homology domain, an ADP-ribosylation factor (Arf)-GTPase-

activating protein (GAP) domain containing a zink finger domain, an ankyrin homology region, a proline-rich region and a C-terminal Src homology 3 (SH3) domain (134). Asap2 is localized in the Golgi apparatus and at the plasma membrane, where it controls Arf-mediated vesicle budding and endocytosis (134,135). In addition, the Asap2 protein is involved in Fcγ receptor-mediated phagocytosis in macrophages (136).

The *ASAP2* gene may be an additional factor in $1,25(OH)_2D_3$-mediated modulation of the immune system. However, due to the presence of multiple protein-protein interaction domains, not all cellular functions of the Asap2 protein are characterized and therefore the role of $1,25(OH)_2D_3$ in the regulation of such a multi-functional gene may not limit only to immune function.

3 Aims of the Study

The physiological importance of vitamin D_3 signaling is well known. The pleiotropic genomic functions of $1,25(OH)_2D_3$ are mediated through the transcription factor VDR. However, for the majority of genomic VDR binding sites there is no obvious role. Similarly, the mechanistic background of VDR-mediated gene regulation is for most $1,25(OH)_2D_3$ target genes poorly understood.

The general objective of this study was to extend the knowledge about $1,25(OH)_2D_3$-mediated transcriptional regulation through the comparative characterization of a number of its target genes. Therefore, the effects of $1,25(OH)_2D_3$ on a number of example genomic regions were studied using human cell culture models representing breast, fat, monocytes and macrophages. The final goal of this study was to explore the utility of the characterized $1,25(OH)_2D_3$ target genes as biomarkers for evaluating the vitamin D status of human individuals. The more specific aims were as follows:

I To compare at the example of the *IGFBP3* gene the mechanistic differences of $1,25(OH)_2D_3$ and its synthetic analog Gemini on VDR-mediated gene expression.

II To demonstrate the complex and cell-specific role of $1,25(OH)_2D_3$ in the regulation of the genes involved in the regulation of cellular growth, such as *G0S2*, *CDKN1A* and *MYC*.

III To characterize the $1,25(OH)_2D_3$-mediated regulation of the members of the CXCL chemokine cluster on chromosome 4.

IV To describe the VDR-mediated regulation of the *ASAP2* gene in human monocytes and macrophages.

V To extrapolate information of conserved VDR binding sites in adipocytes using the genes *DUSP10* (dual specificity phosphatase 10), *TRAK1* (trafficking protein, kinesin binding 1), *NRIP1* (nuclear receptor interacting protein 1) and *THBD* as examples and to evaluate their use as biomarkers for the vitamin D_3 responsiveness of human individuals.

4 Materials and Methods

4.1 MATERIALS

4.1.1 Cell culture

The human non-tumorigenic mammary epithelial cell line MCF-10A, which was used in study I, is a spontaneously immortalized estrogen receptor negative cell line, which was derived from a mammary tissue of a 36-year-old female with cystic fibrosis (137). Adherent MCF-10A cells were grown in a mixture of Dulbecco's Modified Eagle's Medium and Ham's F12 medium 1:1 (DMEM/F12 (1:1)) supplemented with 20 ng/ml epidermal growth factor, 100 ng/ml cholera toxin, 10 μg/ml insulin, 500 ng/ml hydrocortisone, 0.1 mg/ml streptomycin, 100 U/ml penicillin and 5% horse serum. Prior to mRNA and ChIP experiments the cells were seeded overnight in medium with 5% charcoal-stripped fetal bovine serum (FBS) instead of horse serum and reached a density of 50 to 60% confluence. FBS had been stripped of lipophilic compounds by stirring with 5% (w/v) activated charcoal for 3 h at room temperature. Charcoal was then removed by centrifugation and sterile filtration (0.2 mm pore size).

The human prostate epithelial cell line RWPE-1, which was also used in study I, had been derived from a histologically normal prostate of a healthy 54-year-old male (138). Adherent RWPE-1 cells were cultured in keratinocyte serum free medium supplemented with 2 mM L-glutamine, 5 ng/ml human recombinant epidermal growth factor, 0.05 mg/ml bovine pituitary extract, 0.1 mg/ml streptomycin and 100 U/ml penicillin. Prior to mRNA experiments the cells were grown for 72 h to reach a density of 45 to 60% confluence.

The human monocytic leukemia cell line THP-1, which as used in studies II, III and IV, was derived from acute myeloid leukemia of a one year old male (139). Suspension THP-1 cells were grown in Roswell Park Memorial Institute medium (RPMI) 1640 medium supplemented with 2 mM L-glutamine, 0.1 mg/ml streptomycin, 100 U/ml penicillin and 10% FBS. Prior to mRNA and ChIP experiments, THP-1 cells were seeded overnight in a density of 500,000 cells/ml (II, III) or 500,000 to 650,000 cells/ml (IV) in phenol red-free RPMI 1640 medium supplemented with 5% charcoal-stripped FBS, 2 mM L-glutamine, 0.1 mg/ml streptomycin and 100 U/ml penicillin.

Suspension grown THP-1 monocytes can be differentiated into adherent M2-type macrophage-like cells using PMA (39). For differentiation THP-1 cells were seeded in a density of 500,000 cells/ml for 72 h in RPMI 1640 medium supplemented with 2 mM L-glutamine, 0.1 mg/ml streptomycin, 100 U/ml penicillin, 10% FBS and 20 nM PMA. During mRNA and ChIP experiments, non-differentiated (non-adherent) cells were washed off with phosphate-buffered saline (PBS).

The human pre-adipocyte cell line SGBS, which as used in study V, had been derived from an adipose tissue specimen of a male infant with Simpson-Golabi-Behmel syndrome (140). Adherent SGBS cells were grown in DMEM/F12 (1:1) supplemented with 8 μg/ml biotin, 4 μg/ml pantothenate, 2 mM L-glutamine, 0.1 mg/ml streptomycin, 100 U/ml penicillin and 10% FBS. All cell culture flasks or plates were coated with a solution of 10 μg/ml fibronectin and 500 μg/ml gelatin in PBS. Prior to mRNA and ChIP experiments, cells were seeded overnight in phenol red-free DMEM/F12 (1:1) supplemented with 5% charcoal-stripped FBS, 8 μg/ml biotin, 4 μg/ml pantothenate, 2 mM L-glutamine, 0.1 mg/ml streptomycin and 100 U/ml penicillin.

All cells were grown in a humidified 95% air / 5% CO_2 incubator at 37 °C. During the experiments, the cells were treated with $1,25(OH)_2D_3$ (10 nM final concentration diluted with 0.001% ethanol (I, II, III and IV-PMA cells), 100 nM final concentration diluted with 0.1% ethanol (IV-THP-1 cells) or 100 nM final concentration diluted with 0.01% ethanol

(V)), Gemini (10 nM final concentration diluted with 0.001% ethanol) or solvent (0.001% ethanol (I, II, III and IV-PMA cells), 0.1% (IV-THP-1 cells) or 0.01% (V)).

4.1.2 Samples of the VitDmet study

73 individuals participating to the VitDmet study (NCT01479933, ClinicalTrials.gov) from the region of Kuopio, Finland (63 °N) were supplemented during 5 winter months with placebo, 40 or 80 μg vitamin D_3. The individuals were selected to be ≥ 60 years of age with evidence of disturbed glucose homeostasis, i.e. impaired fasting glucose or impaired glucose tolerance, but no type 2 diabetes, and had a BMI between 25 and 35. The research ethics committee of the Northern Savo Hospital District had approved the study protocol (#37/2011). All participants gave a written informed consent to participate in the study. Needle biopsies (0.5-1 g) from subcutaneous abdominal adipose tissue were taken from 47 individuals (17, 14 and 16 individuals supplemented with placebo, 40 or 80 μg vitamin D_3, respectively) under local anesthesia (10 mg/ml lidocaine without adrenalin) at the beginning and the end of the study. The samples were washed twice with PBS, snap frozen in liquid nitrogen and stored at -80 °C until used for RNA extraction.

Serum 25(OH)D_3 concentrations were measured from venous blood samples using a high performance liquid chromatography with coulometric electrode array (141). The blood samples for determining the 25(OH)D_3 concentrations were collected at the same time as the adipose samples. The serum 25(OH)D_3 concentrations of the 47 investigated study participants varied at the beginning of the study between 35.9 and 73.6 nM and increased in average by 20.8 nM. The measurement of other basic clinical and biochemical variables showed that neither the BMI nor the serum calcium concentrations significantly changed during the intervention.

4.2 METHODS

4.2.1 RNA extraction, cDNA synthesis and qPCR

Cultured cells were stimulated for indicated time periods and total RNA was extracted using the High Pure RNA Isolation Kit (Roche) or the Quick RNA Miniprep Kit (Zymo Research) following manufacturer's instructions. Total RNA amount was quantified with a NanoDrop ND-1000 spectrophotometer. cDNA synthesis was performed with the Transcriptor First Strand cDNA Synthesis Kit (Roche) using 1 μg (I, II, III, IV) or 500 ng (V) of total RNA as a template. RNA was pre-denaturated for 10 min with oligo $(dT)_{18}$ primers at 65 °C and reverse transcription was carried out for 30 min at 55 °C following final denaturation for 5 min at 85 °C, before the samples were diluted to 400 μl with nuclease free water.

Total RNA from primary adipose samples (V) was extracted using the TRIzol method followed by further purification using the miRNeasy Mini Kit (Qiagen). RNA was reverse transcribed into cDNA using the High-Capacity cDNA Archive Kit (Applied Biosystems) following manufacturer's instructions.

Real-time quantitative polymerase chain reaction (qPCR) of cDNA templates were performed with the LightCycler 480 System (Roche) using 250 to 400 nM of reverse and forward primers and the LightCycler 480 SYBRGreen I Master mix (Roche), Maxima SYBR Green/Fluorescein qPCR Master Mix (Fermentas) or Maxima SYBR Green/ROX qPCR Master mix (Fermentas). Hotstart Taq polymerase was activated for 10 min at 95 °C, followed by 42 to 45 amplification cycles of 20 s denaturation at 95 °C, 15 to 20 s annealing at primer-specific temperatures and 15 to 20 s elongation at 72 °C, and a final elongation for 10 min at 72 °C. PCR product specificity was monitored using post-PCR melt curve analysis. Relative expression levels were determined for each sample separately relative to the reference gene ribosomal protein, large, P0 (*RPLP0*) (I, III) or to the mean of the expression levels of the reference genes β2 microglobulin (*B2M*), glycerinaldehyde-3-

phosphate-dehydrogenase (*GAPDH*) and hypoxanthine phosphoribosyltransferase 1 (*HPRT1*) (II, IV), or *RPLP0* and *GAPDH* (V) using the formula $2^{-(\Delta Ct)}$, where ΔCt is $Ct_{(target\ gene)}$ – mean of $Ct_{(reference\ genes)}$. To measure the effect of $1,25(OH)_2D_3$ stimulation, relative mRNA expression levels in ligand-treated samples were compared against solvent treated control samples to obtain fold change values.

4.2.2 ChIP

After treatment of cells, nuclear proteins were cross-linked to DNA by adding formaldehyde directly to the medium to a final concentration of 1% and incubating for 5 to 10 min at room temperature on a rocking platform. Cross-linking was stopped by adding glycine to a final concentration of 0.125 M and incubating at room temperature for 5 min on a rocking platform. Adherent cells were washed with ice-cold PBS and scraped either into PBS (I) or into Farnham Lysis buffer (0.5% NP-40, 85 mM KCl, protease inhibitors, 5 mM PIPES, pH 8.0, III, IV and V) and then pelleted by centrifugation. Suspension cells were collected, washed with ice-cold PBS and then pelleted. The cell pellets were resuspended in lysis buffer (1% SDS, 10 mM EDTA, protease inhibitors (Roche), 50 mM Tris-HCl, pH 8.1) and the lysates were sonicated using a Bioruptor UCD-200 (Diagenode, I) or a Bioruptor Plus (Diagenode, II to V). Cellular debris was removed by centrifugation and the lysates were diluted 1:10 in ChIP dilution buffer (0.01% SDS, 1.1% Triton X-100, 1.2 mM EDTA, 167 mM NaCl, protease inhibitors, 250 μg/ml BSA, 16.7 mM Tris-HCl, pH 8.1) to obtain output samples (immunoprecipitated DNA). For input samples, the lysates were diluted 1:10 in ChIP dilution buffer without protease inhibitors and BSA.

In study I, one μg of antibodies against VDR (sc-1008), HDAC4 (sc-11418) or HDAC6 (sc-11420), all from Santa Cruz Biotechnology, or acetylated histone H4 (06-866) or non-specific IgG (12-370), both from Millipore, were added to output samples and chromatin solutions were incubated overnight at 4 °C with rotation. The immuno-complexes were collected with 60 μl of protein A agarose beads (Millipore) for 1 h at 4 °C with rotation. In the studies II to V, one μg of antibodies against VDR (sc-1008, Santa Cruz Biotechnology), CCCTC-binding factor (CTCF, 07-729, Millipore, III) or non-specific IgG (12-370, Millipore) were pre-bound to 20 μl of Magna ChIP Protein A Magnetic Beads (Millipore) or 60 μl of protein A agarose beads (Millipore, IV-THP-1 cells) in 3 h to overnight incubations at 4 °C with rotation. The formed bead-antibody complexes were washed with ChIP dilution buffer and added to the output samples. The samples were incubated overnight at 4 °C with rotation to form the immuno-complexes.

The immuno-complexes were then washed sequentially for 4 min with the following buffers: low salt wash buffer (0.1% SDS, 1% Triton X-100, 2 mM EDTA, 150 mM NaCl, 20 mM Tris-HCl, pH 8.1), high salt wash buffer (0.1% SDS, 1% Triton X-100, 2 mM EDTA, 500 mM NaCl, 20 mM Tris-HCl, pH 8.1) and LiCl wash buffer (0.25 M LiCl, 1% Nonidet P-40, 1% sodium deoxycholate, 1 mM EDTA, 10 mM Tris-HCl, pH 8.1). Finally, the immuno-complexes were washed twice with TE buffer (1 mM EDTA, 10 mM Tris-HCl, pH 8.1, I or pH 8.0, II to V). DNA was eluted from the beads with buffer (25 mM Tris-HCl, pH 7.5, 10 mM EDTA, 0.5% SDS) in a 30 min incubation at 65 °C (I) or with buffer (1% SDS, 100 mM $NaHCO_3$) in two 15 to 20 min elutions at room temperature with rotation (II to V). The output and input samples were reverse cross-linked at 64 to 65 °C for 5 h to overnight in the presence of proteinase K (Fermentas, I or Roche, II to V). The DNA was isolated either with the ChIP DNA Clean & Concentrator Kit (Zymo Research) or with phenol/chloroform/isoamyl alcohol (25:24:1) extraction followed with precipitation using 0.1 volume of 3 M sodium acetate, pH 5.2, and 2 volumes of ethanol with glycogen as carrier. DNA concentrations were determined by Quant-iT PicoGreen dsDNA Assay Kit (Invitrogen).

4.2.3 qPCR of chromatin templates

Genomic primers were designed for the VDR or CTCF binding regions examined in these studies. As control regions, where neither VDR nor CTCF binding was observed, a region

located 46 kb upstream of the *CDKN1A* gene (II, III) or a region located at exon 2 of the myoglobin (*MB*) gene (IV, V) were used. In study I, 5'-end 6-carboxyfluorescein and 3'-end Black Hole Quencher 1 labeled hydrolysis probes (Eurogentec) were used. Selected genomic regions were analyzed with qPCR using the LightCycler 480 System (Roche) with 400 nM of reverse and forward primers, 25 nM amplicon-specific probes and the Maxima Probe qPCR master mix (Fermentas). Hotstart Taq polymerase was thermally activated for 10 min at 95 °C, followed by 50 amplification cycles of 20 s at 95 °C and 60 s at 60 °C. The PCR product specificity was monitored using 2% agarose gels. In studies II to V, selected genomic regions were analyzed with qPCR using the LightCycler 480 System (Roche) with 250 to 400 nM of reverse and forward primers and the LightCycler 480 SYBRGreen I Master mix (Roche). Again the hotstart Taq polymerase was activated with a 10 min at 95 °C step, followed by 43 to 45 amplification cycles of 20 s denaturation at 95 °C, 15 s annealing at primer-specific temperatures and 15 s elongation at 72 °C, and a final elongation for 10 min at 72 °C. PCR product specificity was monitored using post-PCR melt curve analysis.

Relative association of chromatin-bound protein or histone modifications were normalized with respect to the corresponding input using the formula $E^{-(\Delta Ct)}$ x100%, where E is amplification efficiency and ΔCt is $Ct_{(output)} - Ct_{(input)}$, output is the immuno-precipitated DNA and input is the purified genomic DNA.

4.2.4 ChIP-seq, FAIRE-seq and ChIA-PET data visualization

Genome-wide ChIP-seq, FAIRE-seq and chromatin interaction analysis with paired-end tag sequencing (ChIA-PET) data was visualized for the studied regions (II to V) to get an overview of the VDR and CTCF binding sites, active or accessible chromatin and chromatin interactions, respectively. Publically available data obtained from undifferentiated THP-1 cells were used for VDR ChIP-seq (GSE27437, II, III, IV) and FAIRE-seq (GSE40075, II, III). VDR ChIP-seq data from PMA-differentiated THP-1 cells (GSE51181) was obtained during this thesis project (II, III, IV). In study V, data from the harmonized analysis of six publically available VDR ChIP-seq datasets was used (GSE53041). The harmonized analysis contained VDR ChIP-seq data from undifferentiated THP-1 cells, LPS-differentiated THP-1 cells, lymphoblastoid cells GM10855 and GM10861, hepatic stellate cells LX2 and colorectal cancer cells LS180. All of the above mentioned data sets are available at GEO (www.ncbi.nlm.nih.gov/geo).

Publically available datasets of the ENCODE consortium (142) were downloaded from UCSC (http://genome.ucsc.edu/ENCODE). ChIP-seq data were downloaded for CTCF (III, IV) and histone 3 lysine 4 methylation (H3K4me) (IV) from K562 human monocytic leukemia cells (CTCF, wgEncodeEH002279; H3K4me, wgEncodeEH000400), from human umbilical vein endothelial cells (HUVEC; CTCF, wgEncodeEH000054; H3K4me, wgEncodeEH000412) and from normal human epidermal keratinocytes (NHEK; CTCF, wgEncodeEH000063; H3K4me, wgEncodeEH000068). ChIA-PET data were downloaded for CTCF-mediated chromatin loops in K562 cells (wgEncodeEH002075, II, III, IV).

The Integrative Genomics Viewer (IGV) (143) was used to visualize ChIP-seq and FAIRE-seq data and the UCSC genome browser (144) was used to visualize the ChIA-PET data.

4.2.5 siRNA inhibition

In study I, mRNA expression of the genes *HDAC4* and *HDAC6* was inhibited by transfecting MCF-10A cells with siRNA oligonucleotides using Lipofectamine RNAiMAX reagent (Invitrogen). The positive surface charge of the reagent mediates interactions between the siRNAs and the cell membrane, allowing the oligonucleotides to enter the cell. Three specific double-stranded siRNA oligonucleotides against the target gene were used simultaneously (200 pmol of each) while a single unspecific double-stranded oligonucleotide served as a control (600 pmol). The siRNAs were diluted in 500 µl cell culture medium without antibiotics and serum. 5 µl RNAiMAX reagent was added and the mixture was incubated for 15-20 min at room temperature. MCF-10A cells (350,000) and the

oligonucleotide solution were combined in 2.5 ml cell culture medium without antibiotics and with horse serum (5% final concentration). Transfected cells were grown 24 h before ligand treatment.

The efficiency of siRNAs to inhibit mRNA expression was measured with qPCR and silencing at the protein level was verified by western blot analysis using 25 μg of whole cell extract. Cellular proteins were separated on 12% SDS polyacrylamide gels and the blotted proteins were detected using specific primary antibodies (see chapter 4.2.2 ChIP) or anti-β-actin antibody (Sigma-Aldrich) as a loading control. DyLight 800 conjugated anti-primary secondary antibodies (Thermo Scientific) were used to detect primary antibodies. Emissions from the conjugated fluorophores on the secondary antibodies were detected with an Odyssey reader (Li-Cor Biotechnology).

4.2.6 Correlation analysis

In study V, the participants of the VitDmet trial were ranked according to their responsiveness to vitamin D_3. The ranking was done under the assumption of a linear positive correlation between the changes of the mRNA expression of the four studied target genes, *DUSP10*, *TRAK1*, *NRIP1* and *THBD*, and the alterations in the serum 25(OH)D_3 concentrations. The ranking was performed for each target gene separately. First, the study participants were sorted, in ascending order, according to their ratios between the changes of the gene expression and serum 25(OH)D_3 concentration. Next, starting from the mean, individuals were ranked both in ascending and descending order for each VDR target gene. Finally, for values of equal rank the distance of the value to the mean determined the final ranking.

Linear regression analysis between changes in gene expression and serum 25(OH)D_3 concentration was performed using Microsoft Excel, versions 2010 and 2011.

5 Results

5.1 DYNAMIC REGULATION OF 1,25(OH)$_2$D$_3$ TARGET GENES

The *IGFBP3* gene has been identified as a primary 1,25(OH)$_2$D$_3$ target gene in prostate cancer cells (36,93). In addition, gene regulation by a number of NRs has been shown to follow a dynamic pattern (76,77). To find out whether *IGFBP3* is a 1,25(OH)$_2$D$_3$ target gene also in mammary cells and to evaluate the dynamics of its transcription, 15 min interval 1,25(OH)$_2$D$_3$ treatments were performed using MCF-10A, an immortalized normal human mammary epithelial cell line. The *IGFBP3* gene was up-regulated dynamically by 1,25(OH)$_2$D$_3$, while its up-regulation by the synthetic vitamin D analog Gemini was not fluctuating (I, Figure 1). In addition, the induction of the *IGFBP3* gene in response to Gemini treatment was more potent, showing a 5.5-fold up-regulation after 240 min treatment, while 1,25(OH)$_2$D$_3$ stimulation caused only a 2.6-fold induction.

Previous studies have characterized two VDR binding sites within the *IGFBP3* promoter, which are called RE1/2 and RE3 (36,93). ChIP analysis of VDR binding showed parallel cyclical VDR association on the both VDR binding sites in response to 1,25(OH)$_2$D$_3$ (I, Figure 2). In contrast, after Gemini treatment, VDR binding to these regions was more linear. In addition, Gemini induced more VDR binding on RE3 at all measured time points, while on RE1/2 the ligand-induced maximal VDR binding was stronger after 1,25(OH)$_2$D$_3$ treatment.

Interestingly, from all 11 human *HDAC* genes only *HDAC4* and *HDAC6* respond to 1,25(OH)$_2$D$_3$ treatment in a dynamic fashion, while no up-regulation of the genes was observed in response to Gemini (I, Figure 3). The association of HDAC4, HDAC6 and chromatin activation measured by histone 4 acetylation was analyzed by ChIP, in order to study the dynamics of a physical HDAC association with the two VDR binding sites of the *IGFBP3* promoter. Strong HDAC4 binding was found to coincide with low VDR binding at the same time point. Both ligands induced the reduction in HDAC4 and HDAC6 binding after 15 to 45 min treatment. To evaluate the hypothesis that transcriptional cycling of the *IGFBP3* gene originates from the actions of HDAC4 and HDAC6, a simultaneous silencing of *HDAC4* and *HDAC6* mRNA expression was performed. After the knock-down of both genes, the cyclical up-regulation of the *IGFBP3* gene by 1,25(OH)$_2$D$_3$ diminished (I, Figure 5) suggesting that the dynamic response of the *IGFBP3* gene is based on a cyclical association of VDR, HDAC4 and HDAC6 on the gene promoter.

Transcriptional cycling of the gene *IGFBP3* was not observed in human RWPE-1 prostate epithelial cells (I, Figure S2). Furthermore, in studies II to IV, which were performed in THP-1 monocytic cell line models, no similar cycling of mRNA levels of primary 1,25(OH)$_2$D$_3$ target genes that were investigated in these studies was detected (II, Figure 1; III, Figures 2B-D and 4B-D; IV, Figures 1D and E). Some of the genes showed a non-continuous up-regulation, such as *CDKN1A* (II, Figure 1B), *CXCL6* (III, Figure 2C) and *CXCL1* (III, Figure 2D), but all mRNA time course experiments had been performed using 30 min intervals and showed relatively high variation. Therefore, monitoring cyclical events remains challenging. In study V, primary 1,25(OH)$_2$D$_3$ target genes were studied in human SGBS pre-adipocytes with 60 min intervals, therefore possible cycling could not be detected. In addition, no time course ChIP experiments were performed in studies II to V. Therefore, the dynamic association of VDR on the regulatory region of these target genes has not yet been investigated.

5.2 VDR BINDING PROFILE IN THE REGIONS OF STUDIED $1,25(OH)_2D_3$ TARGET GENES

Primary target gene activation by $1,25(OH)_2D_3$ is mediated exclusively via VDR binding upstream or downstream of the target gene's TSS. The genome-wide analysis of VDR binding sites has revealed a large variation in the distance of VDR binding sites from the target gene's TSS, in the number of VDR binding sites within the genomic region of the target gene and in the number of target genes that are regulated by the same VDR locus (81). In addition, a harmonized analysis of six different VDR ChIP-seq datasets (71) demonstrated that most VDR binding sites are cell type-specific. Therefore, it is essential to create a general view on the VDR binding profile in the used cellular model, in order to understand the effects of $1,25(OH)_2D_3$ on the studied genomic region.

The size of the chromosomal regulatory domains can be estimated by DNA looping mediated by the transcription factor CTCF (145). The high conservation of genomic CTCF binding sites (146) allows a reliable extrapolation of CTCF ChIP-seq data from K562 cells, which are also human monocytic leukemia cells (147), to THP-1 cells. Publicly available genome-wide CTCF ChIP-seq and CTCF ChIA-PET data (142), which were obtained from K562 cells, were used to evaluate the size of the chromosomal region around VDR binding sites. In addition, conservation of the CTCF binding was confirmed by using the ChIP-seq data derived from HUVEC and NHEK cells, which are far more distinct from THP-1 cells than K562 cells. The information about DNA looping, derived from ChIA-PET data (II, III, IV), as well as CTCF binding data derived from ChIP-seq data (III, IV), were used to assess the size of the VDR-regulated chromosomal domain. Additionally, the binding of CTCF to sites, which were described in public datasets, was confirmed in monocytes by ChIP-qPCR (III, Figure 1B). In order to have a general view on the VDR binding profile in the used THP-1 cell models (II, III, IV), i.e. monocytes (non-differentiated) and macrophages (PMA-differentiated), VDR ChIP-seq data were obtained (macrophages) or taken form a previously published study (monocyte (81)) and used in the visualizations.

The visualization of VDR binding data revealed that the genomic regions around the three investigated cancer-associated $1,25(OH)_2D_3$ target genes, *G0S2*, *CDKN1A* and *MYC*, contained one to four VDR binding sites. Only some of these sites carried a DR3-type motif (II, Figure 2). The genomic region surrounding the *G0S2* gene contains only one VDR peak with a DR3-type motif, which was active both in monocytes and macrophages (II, Figure 2A). In contrast, in the region of the *CDKN1A* gene three active VDR binding sites, of which two carry a DR3-type sequence, were active in monocytes, but none of them were occupied in macrophages (II, Figure 2B). Moreover, in the region of the *MYC* gene from the four VDR binding sites that were observed in monocytes, only the two that contain a DR3-type motif were used in macrophages (II, Figure 2C). In study III, the isolated genomic region around the CXCL chemokine cluster was found to contain only one VDR binding locus (carrying a DR3-type motif) in monocytes that was occupied also in macrophages (III, Figure 5A). In contrast, the prominent primary $1,25(OH)_2D_3$ target gene *ASAP2* was activated both in monocytes and macrophages by three VDR binding sites (IV, Figure 2A), all of which contain a DR3-type binding motif.

Taken together, all studied chromosomal domains have individual VDR binding characteristics concerning the number of active VDR binding loci with and without a DR3-type binding motifs.

5.3 $1,25(OH)_2D_3$ TARGET GENES IN MONOCYTES AND MACROPHAGES

5.3.1 Cancer-associated $1,25(OH)_2D_3$ target genes

In study I the regulatory mechanism of the VDR-mediated up-regulation of the *IGBFP3* gene was established in MCF-10A normal human mammary cells. IGFBP3 has important

anti-cancer functions in breast cancer and a significant role in 1,25$(OH)_2D_3$-induced apoptosis (34). To increase the knowledge of 1,25$(OH)_2D_3$-mediated growth inhibition in THP-1 myelomonocytic leukemia cell models, three known cancer-associated 1,25$(OH)_2D_3$ target genes, *G0S2*, *CDKN1A* and *MYC*, were selected for study II. In both undifferentiated THP-1 cells (monocytes) and PMA-differentiated THP-1 cells (macrophages) the *G0S2* gene was shown to be an up-regulated primary 1,25$(OH)_2D_3$ target, being significantly induced after 1 h of ligand treatment (II, Figure 1A). Although the basal mRNA expression of the *G0S2* gene was higher in macrophages, the gene showed far stronger inducibility in macrophages than in monocytes (5.3-fold and 2.6-fold inductions, respectively, after 8 h of ligand treatment) (II, Figures 1A and S1). The gene *CDKN1A* showed a faint but significant response to 1,25$(OH)_2D_3$ treatment in both cellular models (II, Figure 1B). The up-regulation was significant 2.5 h after ligand treatment in both cell types but the maximal induction was only 1.6-fold in monocytes and even as low as 1.3-fold in macrophages. The basal mRNA expression level of the *CDKN1A* gene was about the same in both cell types. In contrast to the up-regulation of the genes *G0S2* and *CDKN1A*, the *MYC* gene showed slight tendency towards down-regulation in monocytes (II, Figure 1C). Interestingly, when the cells were differentiated to macrophages, *MYC* turned out to be an early responding up-regulated 1,25$(OH)_2D_3$ target gene. Differentiation reduced basal mRNA expression level of the gene as well.

In order to estimate the number of VDR binding sites around the genes *G0S2*, *CDKN1A* and *MYC*, the sizes of the chromosomal regulatory domains containing the respective genes were assessed by DNA looping mediated by the insulator protein CTCF (based on CTCF ChIA-PET data (142); II, Figure S3). Visualization of VDR ChIP-seq data from monocytes (81) and macrophages showed that the genomic region containing the *G0S2* gene, which is at maximum 180 kb of size, contains only one VDR binding site located 15 kb upstream of the gene's TSS (II, Figures 2A and S3A). The VDR binding site is active both in monocytes and macrophages and is contained within all possible CTCF-mediated DNA loops (II, Figures 2A and S3A). In addition, the site has a significant level of accessible chromatin, as determined by FAIRE-seq (86), which is further induced in response to 1,25$(OH)_2D_3$ treatment (II, Figure 3). ChIP-qPCR data from monocytes revealed that among all studied VDR binding sites, the site near the *G0S2* gene represents that with the highest inducibility.

The chromatin loops around the *CDKN1A* gene cover 170 kb and contain three VDR binding sites that all are in a region of open chromatin in monocytes (II, Figures 2B and S3B). However, not all the DNA loops contain VDR binding loci 2 and 3. ChIP-qPCR experiment could not confirm the binding of VDR to site 1, although it was suggested by VDR ChIP-seq data. This site has a relatively high rate of open chromatin (II, Figure 3). VDR sites 2 and 3 were ligand-inducible, but site 3 shows higher basal VDR binding. Interestingly, no VDR binding to these or any additional sites was observed in macrophages.

The large chromosomal domain around the *MYC* gene covers 2.8 Mb and contains four VDR binding sites in monocytes (II, Figures 2C and S3C). Open chromatin was observed at VDR loci 2, 3 and 4, of which the latter showed the highest rates of open chromatin among all studied VDR binding sites (II, Figure 3). Interestingly, only the two loci containing DR3-type motifs were occupied also in macrophages. In monocyte ChIP-seq data, VDR binding was down-regulated in response to 1,25$(OH)_2D_3$ treatment at site 1, which is the only site without open chromatin among all studied sites. This down-regulation was however not observed after one hour treatment in the ChIP-qPCR experiment, although strong basal VDR binding was found (II, Figure 3).

In summary, the observed diversity of mRNA inductions in the studied genes, is originating from the unique VDR binding profile to the respective regulatory regions of the three studied genes. In addition, in the genomic regions of the genes *CDKN1A* and *MYC* the enrichment of VDR is cell type specific.

5.3.2 The CXCL gene cluster

The CXCL gene cluster on chromosome 4 contains nine genes encoding the chemokines CXCL1 to CXCL8 and CXCL4.1. Analysis of previously published VDR ChIP-seq and microarray data (81) suggested the *CXCL8* gene as a $1,25(OH)_2D_3$ target in THP-1 monocytes. The gene *CXCL8*, also known as *IL8*, is a major neutrophil chemoattractant and was the first identified chemokine (124,130). The responsiveness of *CXCL8* to $1,25(OH)_2D_3$ gave initiation to study III, in which the impact of $1,25(OH)_2D_3$ on the regulation of the whole CXCL chemokine cluster was investigated. Visualization of publicly available data for CTCF ChIP-seq and CTCF ChIA-PET (142) and a ChIP-qPCR analysis for CTCF binding suggested that the whole CXCL gene cluster, but not any other gene, belongs to the same chromosomal domain that is isolated by bordering CTCF sites (III, Figure 1). Interestingly, visualization of FAIRE-seq data from monocytes (86) indicated high rates of accessible chromatin in the region spanning the genes *CXCL8*, *CXCL6*, *CXCL4.1* and *CXCL1* (III, Figure 1A).

VDR ChIP-seq analysis in THP-1 monocytes highlighted a prominent $1,25(OH)_2D_3$-inducible VDR binding site between the genes *CXCL6* and *CXCL8*, located 22 kb downstream of the *CXCL8* TSS (III, Figures 1A and 3A). In addition, VDR ChIP-seq data from PMA-differentiated THP-1 macrophages (III, Figure 5A) showed that this site is ligand-inducible also in macrophages. VDR binding and inducibility in response to $1,25(OH)_2D_3$ was confirmed by ChIP-qPCR experiments performed in monocytes and macrophages (III, Figures 3B and 5B, respectively). Furthermore, FAIRE-seq data indicated that the VDR locus is accompanied with accessible chromatin (III, Figure 3A). In addition, FAIRE-seq time course data revealed ligand-inducible chromatin opening at this site in monocytes.

To gain an overview on the whole CXCL gene cluster, relative basal mRNA expression levels of the genes of the cluster and its flanks were measured by qPCR. In monocytes, only the genes *CXCL1*, *CXCL6* and *CXCL8* were expressed (III, Figure 2A). All three genes are up-regulated primary $1,25(OH)_2D_3$ target genes that display significant induction already 1 h after stimulation (III, Figures 2B-D). *CXCL8* demonstrated highest basal expression accompanied with most pronounced inducibility, 9.1-fold after 8 h $1,25(OH)_2D_3$ stimulation, of the three genes. No induction of the flanking genes was observed. The basal expression of the CXCL cluster in macrophages indicated two additional genes, *CXCL3* and *CXCL7*, but neither of them responded to $1,25(OH)_2D_3$ treatment (III, Figures 4A and S2). In macrophages, the gene *CXCL8* showed a 33-fold increased basal expression, while only slightly higher basal expression levels of *CXCL1* and *CXCL6* were observed when compared to monocytes (III, Figure 4). Although all three genes were primary $1,25(OH)_2D_3$ targets also in macrophages, they exhibited delayed response to $1,25(OH)_2D_3$ stimulation and showed attenuated maximum induction compared to monocytes (III, Figures 4B-D). For example, the first significant induction of the *CXCL8* gene was detected 3.5 h after $1,25(OH)_2D_3$ stimulation and even 8 h after the induction with hormone was only 1.9-fold.

Taken together, $1,25(OH)_2D_3$ regulates specifically the expression of the inflammatory cytokine genes *CXCL1*, *CXCL6* and *CXCL8* in both monocytes and macrophages. However, the induction is reduced in macrophages, where the basal expression of the genes is higher.

5.3.3 The *ASAP2* gene

Analysis of the previously published VDR ChIP-seq and microarray study in THP-1 monocytes (81) highlighted the genomic region around the *ASAP2* gene containing three strongly inducible VDR binding sites, each of which is carrying a DR3-type motif (IV, Figure 1A). The region around the *ASAP2* gene contains also the genes *ITGB1BP1*, *CPSF3*, *IAH1*, *ADAM17*, *YWHAQ* and *TAF1B*. Publicly available ChIP-seq data for CTCF binding (142) were visualized, in order to evaluate the size of the chromosomal domain around the three VDR binding sites. Using ChIP-seq data for H3K4me (142), CTCF binding sites, which are associated with the gene regulation function and not insulation function, could be

excluded. CTCF binding and ChIA-PET data confirmed that the chromosomal domain around the *ASAP2* gene contains up to three VDR binding sites (IV, Figures 1A and S1). Interestingly, VDR binding data revealed that in response to $1,25(OH)_2D_3$ all three binding sites show a similar pattern of VDR association in monocytes and PMA-differentiated THP-1 macrophages (IV, Figure 2A). Site 2 displayed hormone independent VDR binding, but was also ligand inducible. In contrast, sites 1 and 3 were occupied by the receptor only after $1,25(OH)_2D_3$ stimulation. From the three VDR loci, site 1 exhibited the strongest inducibility in response to $1,25(OH)_2D_3$. VDR ChIP-seq data were confirmed by ChIP-qPCR performed in both monocytes and macrophages (IV, Figure 2B).

With the aim to get a general view on the relative basal mRNA expression profile of the genes in the whole chromosomal domain comprising the three VDR binding sites, qPCR was performed in both monocytes and macrophages (IV, Figure 1B). All genes in the studied region were expressed in both cellular models. However, only the *ASAP2* gene, which displayed rather low expression levels in monocytes, showed a difference in the basal expression levels in comparison of both cellular models, being 77-fold higher expressed in macrophages. In addition, the *ASAP2* gene responded more prominently and faster to $1,25(OH)_2D_3$ treatment in monocytes than in macrophages, reaching a 3.8-fold induction already 2.5 h after ligand stimulation (IV, Figures 1D and E). Furthermore, the *ASAP2* gene was demonstrated to be the only primary target of $1,25(OH)_2D_3$ in the studied genomic region (IV, Figure S2).

In summary, the ligand-induced binding of VDR to the three sites in the studied locus leads to the up-regulation of only one gene, *ASAP2*.

5.4 $1,25(OH)_2D_3$ TARGET GENES IN HUMAN ADIPOCYTES

In study V, primary $1,25(OH)_2D_3$ target genes and VDR binding sites were characterized in the human SGBS pre-adipocyte cell line, for which no VDR ChIP-seq data are available. However, a recent analysis combining all public VDR ChIP-seq datasets indicated 55 conserved VDR binding regions (71) (V, Table S4). Due to the ubiquity in VDR binding in the available cell lines to these sites, these genomic loci are most likely occupied by VDR in SGBS cells. From the 55 VDR loci, four sites located upstream of the genes *DUSP10*, *TRAK1*, *NRIP1* and *THBD* were selected for further investigations (V, Figure 1). Association of VDR with these sites in pre-adipocytes was confirmed by ChIP-qPCR (V, Figure 2). After treatment for 1 and 2 h with $1,25(OH)_2D_3$ the VDR binding was increased at the sites of the genes *DUSP10*, *NRIP1* and *THBD*, whilst the site of the *TRAK1* gene showed VDR binding already in the absence of ligand that was not further induced by ligand treatment. Furthermore, the mRNA expression levels of the genes *DUSP10*, *TRAK1*, *NRIP1* and *THBD* were induced in response to $1,25(OH)_2D_3$ in SGBS cells confirming that these genes are primary $1,25(OH)_2D_3$ target genes and regulated by conserved VDR binding sites located upstream of the genes (V, Figure 3).

In order to increase our understanding about the physiological consequence of the $1,25(OH)_2D_3$ responsiveness of the genes *DUSP10*, *TRAK1*, *NRIP1* and *THBD* in human adipocytes, the expression levels of the genes were studied in human adipose tissues samples, which were obtained by peripheral subcutaneous needle biopsies from 47 participants of the VitDmet study. During this 5-month intervention trial, adipose tissue samples were collected and serum $25(OH)D_3$ concentrations were measured at the start and end of the intervention. The changes in serum $25(OH)D_3$ levels varied between a 2.1-fold decrease and a 2.4-fold increase, while changes in the mRNA expression of the four genes in the adipose tissue samples ranged from a 4.71-fold decrease of *THBD* to a 3.15-fold increase of *NRIP1* (V, Table S1).

The study participants were ranked for each of the four primary VDR target genes separately, assuming a positive correlation between the gene expression level changes and

the respective changes in serum 25(OH)D_3 concentrations during the intervention (V, Table S2). In order to evaluate the assumed correlations, the correlation coefficient (r) was calculated between expression level changes and serum 25(OH)D_3 concentration changes. Study participants were then removed one after the other in reverse order based on their ranking; the r-values were re-calculated again after each step. The r-values and the respective number of remaining study participant were plotted, to identify the number of remaining participants showing an r-value of at least 0.71 ($r^2 > 0.5$) (V, Figure 4). From the four studied genes, *DUSP10* identified 30 participants showing the highest number of individuals among the studied genes. Interestingly, when only the participants with an r-value of at least 0.71 were visualized in correlation graphs, with the exception of one subject, the gene *DUSP10* described the same group of persons (but 7 and 8 additional individuals) as those identified by genes *TRAK1* and *NRIP1* (V, Figure 5).

In summary, the genes *DUSP10*, *TRAK1*, *NRIP1* and *THBD* are primary 1,25(OH)$_2$$D_3$ targets in pre-adipocytes and are regulated by conserved VDR binding sites. The genes can be used as markers for the vitamin D_3 response of human individuals, of which *DUSP10* is the most suitable.

6 Discussion

The secosteroid vitamin D_3 is a pro-hormone involved in a variety of cellular and physiological functions. The active form of vitamin D_3, $1,25(OH)_2D_3$, mediates its biological responses through the NR VDR. VDR binds directly to genomic DNA and regulates target gene expression when activated by ligand. VDR is widely expressed and is the only mediator for the genomic actions of $1,25(OH)_2D_3$. Therefore, characterizing i) tissue-specific genomic VDR locations, ii) molecular actions of VDR regulation on gene expression and iii) tissue-specific VDR target genes is of high impact, in gaining more insight into the physiological function of vitamin D_3.

In the present thesis, the mechanism of the gene regulation by VDR was studied at the example of the gene *IGFBP3*, in order to describe the differences in the mRNA induction while using natural VDR ligand $1,25(OH)_2D_3$ or its synthetic analogue Gemini. In further studies, primary VDR target genes involved in growth inhibition, inflammation and intracellular signaling were characterized in THP-1 monocytes and macrophages. In the final study, conserved VDR target genes were characterized in human pre-adipocytes and the genes were further studied in primary human adipose tissue samples, in order to identify biomarkers representing the vitamin D status of human individuals.

6.1 THE *IGFBP3* GENE IS REGULATED DYNAMICALLY BY $1,25(OH)_2D_3$

In the first part of this thesis (study I), the regulation of the well-known $1,25(OH)_2D_3$ target gene *IGFBP3* was investigated using the cell line MCF-10A. In this study, the previously reported up-regulation (36,93) of the *IGFBP3* gene in response to $1,25(OH)_2D_3$ was confirmed. The ability of $1,25(OH)_2D_3$ to induce *IGFBP3* mRNA 2.5-fold after 4 h treatment was comparable to previously reported results in prostate cancer cell lines (36,93). In response to $1,25(OH)_2D_3$, cyclical mRNA accumulation of the *IGFBP3* gene was demonstrated with phases of RNA synthesis and degradation, with a periodicity of 60 min. In contrast, the synthetic $1,25(OH)_2D_3$ analog Gemini showed linear and stronger (5.5-fold induction after 4 h) up-regulation of the gene. In the previous studies (36,93) the regulation of *IGFBP3* by $1,25(OH)_2D_3$ was studied based on a limited number of time points and therefore transcriptional cycling of *IGFBP3* in these cell lines had not been described. In addition, the observed dynamics in *IGFBP3* mRNA accumulation seems to be cell type specific, since no transcriptional cycling was observed, when the gene was studied under identical conditions in RWPE-1 immortalized prostate cells.

A cyclical induction of a VDR target gene, *CDKN1A*, has been observed earlier in MDA-MB453 breast cancer cells (76). In addition, NR-induced target gene expression was found to include cyclical association of the receptor, RNA polymerase II and co-factors on respective gene promoters (77,78). To have a broader view on the cyclical induction of a VDR mediated transcription, association of VDR, HDAC4 and HDAC6 and chromatin activation were examined in study I on two previously characterized VDR binding regions on the *IGFBP3* promoter. On region 1/2, which is located closer to the gene's TSS, VDR was slightly more prominently associated after $1,25(OH)_2D_3$ treatment when compared to the VDR association induced by Gemini. In addition, the natural VDR ligand induced parallel cyclical VDR association on both regions, while the VDR association in response to Gemini was more linear on both regions. Although in general, lower levels of VDR association were observed on RE3, the binding of VDR was more prominent after Gemini treatment than after $1,25(OH)_2D_3$ stimulation. The observed VDR binding profiles suggest that the Gemini-

induced steady up-regulation of the *IGFBP3* gene is primarily based on the ligand-induced binding of VDR to region 3.

Interestingly, high ligand-induced VDR association corresponded to low HDAC4 association, which suggests that during transcriptional cycling VDR and HDAC4 binding occur in different phases. In addition, the reduction in both HDAC4 and HDAC6 association after 15 to 45 min ligand treatment coincides with an induction of VDR binding at the same time points. Furthermore, in response to $1,25(OH)_2D_3$ the chromatin activation at region 1/2 displayed cycling with similar interval as accumulation of *IGFBP3* mRNA. In addition, changes in HDAC6 association was observed only at region 1/2 in response to $1,25(OH)_2D_3$ treatment, while after Gemini treatment the association of HDAC6 was rather similar with both regions. These observations suggest that the transcriptional cycling of the *IGFBP3* gene is primarily mediated by VDR and chromatin modifier associations at region 1/2.

The observation that *HDAC4* and *HDAC6* are the primary $1,25(OH)_2D_3$ targets but not regulated by Gemini supports the hypothesis that they are important components of $1,25(OH)_2D_3$-mediated cycling of the *IGFBP3* gene. However, it has to be taken into account that the dynamics association of the HDAC4 and HDAC 6 was observed immediately after ligand treatment, and therefore these events cannot result from protein products of the simultaneous mRNA induction of *HDAC4* and *HDAC6*. Nevertheless, the simultaneous silencing of the expression of both *HDAC4* and *HDAC6* resulted in linear *IGFBP3* mRNA accumulation, which confirms the role of both proteins in the $1,25(OH)_2D_3$-mediated transcriptional cycling of the gene.

The study did not analyze the differences in Gemini and $1,25(OH)_2D_3$-induced IGFBP3 protein accumulation. Since treatment with Gemini evokes stronger mRNA accumulation, it can be expected that Gemini induces also higher protein levels compared to that induced by $1,25(OH)_2D_3$. However, the observed transcriptional cycling is most likely not observed as fluctuation of protein levels of IGFBP3 since short temporal changes in mRNA levels are not directly reflecting the protein levels. The physiological impact of transcriptional cycling is rather a feedback loop mechanism for controlling the transcription process. This regulatory mechanism is not used by Gemini.

In conclusion, $1,25(OH)_2D_3$ induces cyclical mRNA induction of the *IGFBP3* gene, which results from sequential association of HDAC4, HDAC6 and VDR to genomic VDR binding loci. For Gemini these mechanisms seem not to apply, and thus the up-regulation of the gene is stronger and linear. This provides mechanistic insight into how $1,25(OH)_2D_3$ and its synthetic analog mediate their growth inhibitory function via *IGFBP3* induction.

6.2 CANCER ASSOCIATED TARGET GENES OF $1,25(OH)_2D_3$

In study II, three genes involved in the control of cellular proliferation, *G0S2*, *CDKN1A* and *MYC*, were selected as examples for demonstrating the complex nature of $1,25(OH)_2D_3$ in the context of growth inhibition. The selection of the genes was based on the evaluation of data from a transcriptome-wide microarray and ChIP-seq experiments prepared in THP-1 monocytic leukemia cells (81). In addition, public ENCODE data were used to estimate the size of the chromosomal domains around the genes.

The response of the *G0S2* gene to $1,25(OH)_2D_3$ was stronger than those of the genes *CDKN1A* and *MYC*. Interestingly, in macrophages the induction of *G0S2* was higher than in monocytes, although the basal expression of the gene increased when the cells differentiated into macrophages. In most cases higher basal expression leads to lower inducibility of the gene, as observed with the genes *CXCL8*, *CXCL6* and *CXCL1* (III) and *ASAP2* (IV). The role of G0S2 protein as a tumor suppressor gene was recently established using the K562 leukemic cellular model (95). Therefore, the finding of study II that *G0S2* is the most induced gene among the examined genes in THP-1 cells suggests that $1,25(OH)_2D_3$

promotes a reasonable proportion of its anti-cancer actions through *G0S2* mRNA induction. However, in THP-1 cells the *G0S2* gene is expressed, thus growth inhibition mediated by G0S2 cannot be directly compared to K562 cells, where it is suppressed (95). In addition, both the role of G0S2 in inhibiting cell proliferation in hematopoietic stem cells (97) and its association with growth arrest of adipocytes (98) are consistent with the observation that the *G0S2* gene is more strongly expressed in macrophages, which do not proliferate anymore. Analysis of VDR ChIP-seq data from monocytes and macrophages indicated that *G0S2* is regulated only by one VDR locus. Interestingly, the same VDR binding site is also occupied in all other publicly available VDR ChIP-seq datasets besides that from colon cancer cells suggesting that the gene is a tissue-wide conserved $1,25(OH)_2D_3$ target.

In macrophages the basal expression of the *CDKN1A* gene was higher than in monocytes but the inducibility by $1,25(OH)_2D_3$ was reduced. In macrophages none of the three VDR binding sites of the gene was occupied suggesting that in these cells the gene is a secondary $1,25(OH)_2D_3$ target. Although VDR association with locus 1 of the *CDKN1A* promoter was observed by VDR ChIP-seq in B cells (82) and in LPS-stimulated THP-1 cells (71), it could not be confirmed by ChIP-qPCR in monocytes. However, the observation of a relatively faint ChIP-seq signal at locus 1 was accompanied by very strong FAIRE-signal (i.e. highly accessible chromatin) in the absence of a DR3-type motif. This suggests that VDR interacts at site 1 with another transcription factor and does not directly bind to DNA. This interpretation fits with the observation form ChIP-qPCR experiments, where such a weak interaction may have not been captured under the used conditions. In contrast, the binding of VDR to the two remaining loci was confirmed by ChIP-qPCR in monocytes.

Evidence from both cell culture and animal models verify that the inhibition of *MYC* expression suppresses cancer cell growth (121). In this study, the observed down-regulation of the *MYC* gene in monocytes suggests that $1,25(OH)_2D_3$ inhibits cellular growth via the *MYC* gene. When monocytes differentiated to macrophages, the repressive effect of $1,25(OH)_2D_3$ on the *MYC* gene changed unexpectedly into an induction. This suggests that in macrophages, which are terminally differentiated, the Myc protein has a different role than in undifferentiated monocytes. Furthermore, the prominent VDR association at site 1 of the *MYC* gene was down-regulated in monocytes in response to $1,25(OH)_2D_3$, which seems to be recovered at 60 min. This dynamic VDR association is supported by the previous observations at the two VDR binding regions on *IGFBP3* promoter (see study I). VDR binding site 1 is located within the coding region of the *MYC* gene, so that temporal three-dimensional chromatin associations of the three remaining VDR binding sites with the transcription machinery may increase the dynamic response observed at site 1. Interestingly, site 1 is not occupied in macrophages, and therefore the regulation of VDR binding to this site may have an important role in triggering the events that switch the down-regulated *MYC* gene in monocytes into up-regulated gene in macrophages. The public VDR ChIP-seq datasets indicate that the four VDR binding sites of the *MYC* gene are only used in THP-1 cells. In contrast to the VDR binding profile in monocytes, VDR ChIP-seq data of LPS-stimulated THP-1 cells (71) suggests that VDR is only associated with sites 2, 3 and 4. Thus, an evaluation whether the *MYC* gene is up- or down-regulated in these cells would give more information about importance of site 1.

The involvement of $1,25(OH)_2D_3$ in the regulation of the three studied $1,25(OH)_2D_3$ target genes controlling cellular growth, *G0S2*, *CDKN1A* and *MYC*, demonstrates, that the hormone has a complex and cell-specific role in growth inhibition of monocytic cells. In monocytes, $1,25(OH)_2D_3$ seems to promote cellular growth inhibition through all these three genes, although the effects on the genes *CDKN1A* and *MYC* are rather modest. For example, dys-regulation of Myc signaling is found in most types of cancers. $1,25(OH)_2D_3$ may simply enhance the transcriptional control of *MYC* expression in monocytes, which is observed as a faint down-regulation in study II. Similarly, if the magnitude of the induction is taken into account, $1,25(OH)_2D_3$ seems to support the functions of p21 in inhibiting the

cell cycle, while the stronger anti-proliferative effects are meditated through the activation of tumor-suppressor gene *G0S2*.

As a primary $1,25(OH)_2D_3$ target, *G0S2* is a rather simple example, as it is strongly induced in both monocytes and macrophages and is controlled by only one VDR binding site close to its TSS region. *G0S2* displays ligand-inducible chromatin opening in its VDR binding site, which is conserved between cell types. While the *CDKN1A* gene is up-regulated in both cell types but demonstrates a rather differential recruitment of VDR to its binding loci, the *MYC* gene reveals significant differences in both mRNA induction and VDR occupancy when monocytes and macrophages are compared. These results propose that each gene has a tissue- and gene-specific complexity in regulation mediated by $1,25(OH)_2D_3$.

6.3 REGULATION OF THE CHEMOKINE CLUSTER ON CHROMOSOME 4 BY $1,25(OH)_2D_3$

Previous VDR ChIP-seq and microarray data from THP-1 monocytes suggested *CXCL8* as primary $1,25(OH)_2D_3$ target gene (81). Therefore, in study III the responsiveness of the whole CXCL chemokine gene cluster to $1,25(OH)_2D_3$ was analyzed both in undifferentiated THP-1 monocytes and in PMA-differentiated macrophages. The study confirmed the *CXCL8* gene as primary up-regulated $1,25(OH)_2D_3$ target gene in monocytes. Moreover, the study described that the neighboring genes *CXCL6* and *CXCL1* were up-regulated as well, whilst no other gene of the cluster was expressed. Moreover, no $1,25(OH)_2D_3$ induction of the expressed flanking genes outside the CXCL cluster was observed. In macrophages the same three CXC genes were up-regulated $1,25(OH)_2D_3$ targets, but showed delayed responsiveness with reduced inducibility. However, the reduced responsiveness is accompanied with higher basal expression and therefore already the lower induction of the genes leads to higher copy numbers of total mRNA synthesis in macrophages than in monocytes.

Analysis of VDR ChIP-seq data from monocytes and macrophages suggested that a single VDR binding site downstream of the *CXCL8* gene regulates the CXCL cluster. In addition, DNA looping mediated by conserved, insulating, CTCF binding sites suggests that all nine CXC chemokine genes belong to the same chromosomal domain. Interestingly, the rather high FAIRE signal in the chromosomal region of the genes *CXCL8*, *CXCL6* and *CXCL1* suggest that in monocytes this region is far more accessible than the remaining CXCL cluster. The *CXCL4.1* gene, which is located between *CXCL6* and *CXCL1*, is a platelet-specific chemokine, which is most likely the reason why it is not expressed in monocytes. However, this study suggests that the *CXCL4.1* gene would be a $1,25(OH)_2D_3$ target gene in tissues where it is expressed. Furthermore, the observation that *CXCL7* and *CXCL3* are expressed in macrophages, but are not induced, suggests that shorter CTCF-mediated regulatory loops, such as a loop from site 2 to site 4, are dominant at least in macrophages.

The observations that i) the VDR binding site is close to the up-regulated genes, ii) it exhibits ligand-dependent chromatin opening, iii) it contains a DR3-type motif and iv) *CXCL8*, *CXCL6* and *CXCL1* are prominently up-regulated after ligand treatment of the cells confirms that these genes are classical $1,25(OH)_2D_3$ target genes. This conclusion is consistent with a recent study (53), where *CXCL8* was found as an up-regulated $1,25(OH)_2D_3$ target in PMA-differentiated THP-1 macrophages. In addition, in that study mycobacterium infection led to the induction of *CXCL8*, which could be further enhanced by stimulation with $1,25(OH)_2D_3$. This suggests that $1,25(OH)_2D_3$ promotes *CXCL8* expression in THP-1 cells even after the gene is induced by PMA or other inflammatory signals. However, the results in THP-1 cells seem to be contradictory to the previous findings (54), which reported that co-treatment with $1,25(OH)_2D_3$ reduced the vast IFN-γ-

mediated induction of *CXCL8* in primary pro-inflammatory monocytes from type 2 diabetes patients. However, the study did not evaluate whether the reduction in *CXCL8* inducibility was a primary or secondary effect of $1,25(OH)_2D_3$. Treatment with IFN-γ stimulates the transcription factor NF-κB, which strongly up-regulates *CXCL8* expression. Since $1,25(OH)_2D_3$ inhibits NF-κB-mediated target gene transcription (48), the contradictory observations may reflect a $1,25(OH)_2D_3$-mediated inhibition of IFN-γ-induced NF-κB transcription rather than a primary effect of VDR on transcription. This is then observed as reduced inducibility of *CXCL8*. In addition, the response of the *CXCL8* gene may depend on the cellular system suggesting that THP-1 cells show different results than primary monocytes.

The general actions of $1,25(OH)_2D_3$ are considered to be anti-inflammatory, so that the observed up-regulation of the inflammatory chemokines on CXCL cluster seems to be a contradiction. However, as the recent study (53) suggested, a supporting role of $1,25(OH)_2D_3$ in chemokine secretion requires also an inflammatory signal. Since $1,25(OH)_2D_3$ is also able to control the inflammatory responses via the repression of NF-κB, the observation in study III suggests that $1,25(OH)_2D_3$ has complex time- and signal-dependent modulatory effects on inflammatory reactions. In addition, the induction by $1,25(OH)_2D_3$ is far lower than that of inflammatory signals, so that the effects of $1,25(OH)_2D_3$ may be only supportive.

In contrast to the observations in study II, where $1,25(OH)_2D_3$ promoted anti-cancer effects in monocytes, the observations from study III suggest that $1,25(OH)_2D_3$ would promote cancer growth through the induction of the angiogenic CXC chemokines in same cells. However, the physiological consequence of transcriptional up-regulation of the inflammatory chemokines in context of cancer is not clear, since their main function is neutrophil chemoattraction. However, the net effect of $1,25(OH)_2D_3$ in this cell line is anti-proliferative despite the up-regulation of angiogenic CXC chemokines.

The findings that both in monocytes and in PMA-differentiated macrophages the genes *CXCL8*, *CXCL6* and *CXCL1* are primary targets of $1,25(OH)_2D_3$ implies a more differential aspect on the modulation of the inflammatory reaction by $1,25(OH)_2D_3$. The study provided more evidence for a role of vitamin D in supporting immune system function.

6.4 THE *ASAP2* GENE LOCUS

Similarly to studies II and III, VDR ChIP-seq and microarray data from THP-1 cells (81) highlighted an interesting genomic region, the *ASAP2* gene locus on chromosome 2, which was further characterized in study IV. In both undifferentiated THP-1 monocytes and PMA-differentiated macrophages the *ASAP2* gene was confirmed as the sole primary $1,25(OH)_2D_3$ target gene of this locus.

The expression levels of all genes within the *ASAP2* locus were characterized in monocytes and macrophages. While the neighboring genes showed constant basal expression levels in both cell types, *ASAP2* mRNA expression increased 80-fold during differentiation from monocytes into macrophages. The responsiveness of the *ASAP2* gene to $1,25(OH)_2D_3$ was reduced in macrophages, where it reached only a 2.6-fold induction after 8 h of treatment. In contrast, in monocytes the gene was more prominently induced already after 2.5 h. The observation that a gene is less induced but has a higher basal expression in the given cellular model, parallels the previous observation concerning the *CXCL8* gene (III). Analysis of VDR ChIP-seq data suggested three VDR binding sites 54, 436 and 574 kb downstream of the *ASAP2* gene, which were confirmed by ChIP-qPCR in both cellular systems. In addition, public data for DNA looping mediated by CTCF (142) indicated that the closest VDR binding site (peak 1, 54 kb downstream) and the *ASAP2* TSS are located on the same chromosomal domain. The VDR binding profile also indicated very high inducibility of VDR binding at that site. Moreover, a larger chromosomal domain

connects *ASAP2* into all three VDR binding sites, but it remains unanswered whether this regulatory loop is used also in THP-1 cells. In the future, VDR ChIA-PET data have to demonstrate VDR-mediated chromatin looping after induction by $1,25(OH)_2D_3$ and will provide more information about the role of the two VDR loci.

None of the *ASAP2* neighboring genes, *ITGB1BP1*, *CPSF3*, *IAH1*, *ADAM17*, *YWHAQ* or *TAF1B*, responded to short term $1,25(OH)_2D_3$ treatment despite the presence of three VDR binding loci in their vicinity. Only after 24 h of $1,25(OH)_2D_3$ treatment there was found to be some minor induction of the genes *IAH1*, *ADAM17* and *YWHAQ* in monocytes suggesting that these genes may be weak secondary targets of $1,25(OH)_2D_3$. However, it is possible that these downstream effects are mediated by primary VDR target genes and may benefit from VDR-induced chromatin opening that would result in increased accessibility of these sites to other transcription factors.

Interestingly, FAIRE-seq data from THP-1 cells (86) demonstrated that all three VDR binding sites within the *ASAP2* region display $1,25(OH)_2D_3$-induced chromatin opening. Genome-wide there are only some 160 of such VDR loci. These VDR binding sites have 2 times more likely a DR3-type motif below their VDR peak summits than average binding sites. Accordingly, all three sites of the *ASAP2* locus contain a DR3-type sequence. This suggests that VDR binding to these sites is more stable than to an average VDR locus. Therefore, these sites may constitute special attraction points for VDR to the genome.

In conclusion, study IV demonstrated that the genomic region around the *ASAP2* gene contains three ligand-inducible DR3-type motif-containing VDR binding sites, which display $1,25(OH)_2D_3$-induced chromatin opening. The study confirmed that the *ASAP2* gene is the only primary $1,25(OH)_2D_3$ target of the three VDR sites both in monocytes and in macrophages.

6.5 VDR BINDING PROFILE RELATED TO REGULATORY DOMAINS IN MONOCYTES AND MACROPHAGES

$1,25(OH)_2D_3$ target genes greatly vary in the size of their regulatory domains formed by CTCF-mediated DNA looping as well as the number of genes and VDR binding loci within these loops. Hence, it is clear that each gene has its customized regulatory scenario mediated by VDR and chromatin organization. For example, in the CXCL cluster, one VDR binding site causes rapid up-regulation of three *CXCL* genes (III), whilst at the *ASAP2* locus three prominent VDR binding sites mediate the up-regulation of only one gene (IV). In contrast, the chromatin loop around the *MYC* gene (II) is about 10 times larger than that of the CXCL cluster or the *ASAP2* locus. However, the chromosomal region around the *MYC* gene contains only a few genes, i.e. it is located within a gene desert area, which is exposed to a variety of regulatory signals. For example, a large number of cancer-associated SNPs are identified in a region located upstream of the *MYC* TSS, which is less than 1 Mb in size (148). SNPs located in this region are among the most important cancer-associated SNPs and affect a large number of cancer cases at the population level (148). The presence of many VDR binding sites at the *MYC* locus, some of which are located fairly distant from the gene's TSS, corresponds with the very pleiotropic regulation of the *MYC* gene.

Furthermore, in the CXCL cluster all expressed genes belong to the same regulatory domain and show similar response to $1,25(OH)_2D_3$ treatment. This means that in that locus, CTCF-mediated regulatory looping seems to determine the target genes of VDR. However, in the *ASAP2* locus six non-responsive genes are expressed in close vicinity of $1,25(OH)_2D_3$ inducible VDR binding loci. The region including most of the non-responsive genes and two VDR binding sites (excluding the *ASAP2* gene and its most inducible VDR site) seems to be located between the main chromatin loops upstream and downstream of the region. This observation suggests that regulatory domains determined by CTCFs are not unambiguous and cannot be applied to predict target genes for all VDR binding sites. In

addition, the two VDR binding sites do not induce any primary response of nearby located genes and are therefore apparently non-functional, despite displaying $1,25(OH)_2D_3$ inducible binding. Unfortunately, the present study could not uncover why VDR is active at these sites.

Future VDR ChIA-PET data will provide a better tool for evaluating chromatin looping and the relation of VDR binding locations to target gene induction. It will demonstrate chromatin looping around VDR in cases where present CTCF data is not applicable. Moreover, it will provide details for the function of single VDR binding sites in cases, which remained undetermined in the projects of this thesis, such as the two distal VDR binding sites of the *ASAP2* locus. Finally, it will provide information about the temporal three dimensional chromatin structure in response to $1,25(OH)_2D_3$ treatment.

6.6 VITAMIN D TARGET GENES IN MONITORING THE VITAMIN D RESPONSE OF HUMAN INDIVIDUALS

Some primary VDR target genes, such as *G0S2* (II), display a similar response to $1,25(OH)_2D_3$ treatment in both monocytes and macrophages, and are regulated by the VDR binding region that is occupied in other cell lines based on public VDR ChIP-seq data. This suggests that these genes are also regulated by the same VDR binding sites in most other tissues. A recent harmonized analysis of all public VDR ChIP-seq experiments (71) resulted in a short list of 55 genomic loci that are occupied by VDR in all these six cell types. In study V, which was performed in human SGBS pre-adipocytes, four genomic regions containing the genes *DUSP10*, *TRAK1*, *NRIP1* and *THBD* were selected as representative examples.

As expected, based on extrapolating the conservation of the VDR binding loci, the study confirmed that the four genes chosen are primary $1,25(OH)_2D_3$ targets as well in the used pre-adipocyte cell model, and regulated by the conserved VDR binding site. Since the genes have been previously identified as primary target genes in monocytes (81), the observation suggests that these conserved VDR target genes are responding to $1,25(OH)_2D_3$ also in most other tissues and cells expressing VDR. As exemplified by the divergent biological function among the four studied genes, *THBD* encoding for an anti-coagulant glycoprotein (149), *TRAK1* coding for an intracellular adaptor molecule (150), *DUSP10* coding for a mitogen-activated protein kinase-specific phosphatase (151) and *NRIP1* coding for a nuclear co-activator (152), $1,25(OH)_2D_3$ has pleiotropic actions in the control of cellular signaling.

Since there is increasing evidence showing that individual responses to vitamin D_3 vary considerably, molecular biomarkers, such as the ubiquitous $1,25(OH)_2D_3$ target genes *DUSP10*, *TRAK1*, *NRIP1* and *THBD*, are needed for the molecular monitoring of the vitamin D status of human individuals. In study V, the assumption that changes in the expression levels of these genes can be used for monitoring vitamin D status was tested with adipose tissue samples of 47 participants of the vitamin D_3 intervention trial VitDmet (NCT01479933, ClinicalTrials.gov). Changes in study participants' serum $25(OH)D_3$ concentrations were compared to the changes in gene expression levels during the intervention. After the study participants were sorted by their responsiveness of gene expression in relation to changes of $25(OH)D_3$ concentration, it was found that the *DUSP10* gene is the most comprehensive biomarker among the investigated genes showing the strongest correlation between the investigated changes. Using *DUSP10* as a marker, 30 out of 47 individuals showed a significant correlation ($r^2>0.5$) between change in serum $25(OH)D_3$ level and change in *DUSP10* expression. When using the genes *TRAK1* and *NRIP1* as markers, the genes identified the same subgroup of individuals as *DUSP10*, but captures with the same correlation threshold ($r^2>0.5$) only 23 and 22 of the 47 study participants, respectively. In contrast, *THBD* expression changes correlated with serum

25(OH)D_3 changes in a different subgroup of participants. From 22 individuals that showed *THBD* response, only 13 were included into the group defined by the three other genes.

In the used pre-adipocyte cell model the *THBD* gene turned out to be more responsive to 1,25(OH)$_2D_3$ treatment than the three other genes examined in the study. Since *THBD* inducibility was also observed in other public datasets, it was selected into the previous study (13), which suggested the genes *THBD* and *CD14* as the most significant single genes associated with the vitamin D status of human individuals. Furthermore, in a study that measured combined *THBD* and *CD14* expression level changes in PBMCs and adipose tissue samples, both genes were used to monitor benefits after vitamin D_3 supplementation (14). However, study V found that the *DUSP10* gene identified more vitamin D_3 responsive individuals than the *THBD* gene and the correlations of all four genes in linear regression analysis showed far higher significance levels than the previous study. This was possible by focusing on highly expressed single genes that were analyzed in only one tissue. Since *THBD* expression in adipose tissue is lower than that of the three other genes, measurements of the latter genes are probably more stable. In addition, genes such as *CYP24A1* that show very high inducibility in pre-adipocytes, are most likely representing rapid changes in their expression levels in biological samples as well. Therefore the genes that show high inductions with low basal expression levels are not the most suitable biomarkers, but rather the modestly induced genes with high basal expression, such observed with *DUSP10*.

The results of study V suggest that individuals, who are characterized by highly induced *THBD* expression, form a distinct group from the responders based on the modestly induced genes *DUSP10*, *TRAK1* and *NRIP1*. This raises the question whether individuals could be categorized into slow and rapid responder groups, based on their target gene response. In order to reliably evaluate this possibility, repeated measurements shortly after vitamin D_3 supplementation are needed. Therefore, further studies will give more statistical power to evaluate the inter-individual variability and allow further categorization of individuals based on their responsiveness to vitamin D_3 supplementation. However, the main observation of study V, demonstrating that some VDR target genes in adipocytes show correlation already within five months between the measuring points, indicates that single target genes can be used as biomarkers for measuring individual vitamin D_3 status.

Among the 30 individuals that showed *DUSP10* response to vitamin D_3, the basal 25(OH)D_3 levels at the start of the intervention varied between 36.9 to 73.6 nM. Interestingly, only 3 of the 30 individuals had the serum 25(OH)D_3 levels below 50 nM which can be considered as insufficiency of vitamin D_3 according IoM (8). The observation suggests that rather the individual's transcriptomic responsiveness to vitamin D_3 supplementation than a fixed serum 25(OH)D_3 level should be considered when vitamin D_3 supplementation is recommended.

Most of the other VDR target genes characterized in this thesis are probably unsuitable as biomarkers. For example, the CXC chemokines (III) are highly and rapidly induced by various inflammatory stimuli. Therefore, most likely the expression changes of these genes represent the individual's inflammatory status. In addition, the cancer-associated primary target genes *MYC* and *CDKN1A* showed differential VDR-mediated transcription already in THP-1 models (II) and therefore the observations may not be applied to other tissues. However, in contrast to *ASAP2* (IV) that is regulated by three VDR binding sites, the primary target *G0S2* (II) is regulated by one conserved VDR binding region and may be suitable for measuring the vitamin D_3 status in tissues where it is expressed.

In conclusion, study V demonstrated a new approach for predicting 1,25(OH)$_2D_3$ target genes based on conservation of genomic VDR binding sites. In addition, it was shown that expression changes of such ubiquitous 1,25(OH)$_2D_3$ targets can be used as molecular biomarkers for the vitamin D_3 responsiveness in human adipocytes and other tissue and cell types.

7 Summary and Conclusion

In this thesis the molecular actions of $1,25(OH)_2D_3$ on several aspects of gene regulation were studied. The main findings of this study can be concluded as follows:

I $1,25(OH)_2D_3$ induces a dynamic and orchestrated mRNA accumulation profile of the *IGFBP3* gene. The dynamic nature of the transcription results from sequential association of HDAC4, HDAC6 and VDR to VDR binding loci leading to repeated induction of *IGFBP3* mRNA production. However, this feedback loop mechanism does not to apply for the induction of the gene by the $1,25(OH)_2D_3$ analog Gemini.

II The example of the genes *G0S2*, *CDKN1A* and *MYC*, which have important functions in cellular growth, established a tissue- and gene-specific scenario in the $1,25(OH)_2D_3$-mediated regulation of the genes. This demonstrates that no single gene is responsible for the control of cellular growth by $1,25(OH)_2D_3$.

III The findings that the chemokine genes *CXCL8*, *CXCL6* and *CXCL1* are primary targets of $1,25(OH)_2D_3$ in both monocytes and macrophages provides more evidence for role of vitamin D_3/$1,25(OH)_2D_3$ in supporting the immune system in its fight against microbes and cancer.

IV The genomic region containing *ASAP2* gene is regulated by three ligand-inducible DR3-type motif-containing VDR binding sites and exhibits $1,25(OH)_2D_3$-induced chromatin opening. The sole function of the VDR regulation at the locus, both in monocytes and in macrophages, is the up-regulation of the *ASAP2* gene.

V Conserved genomic VDR binding sites can be used to predict $1,25(OH)_2D_3$ target genes in other tissues and cell types, as demonstrated for the genes *DUSP10*, *TRAK1*, *NRIP1* and *THBD*. Such ubiquitous $1,25(OH)_2D_3$ targets can be used as molecular biomarkers for evaluating the vitamin D_3 responsiveness of human individuals.

The present study provides further insight into the mechanisms of gene regulation by $1,25(OH)_2D_3$. I demonstrated that the regulation of gene expression by $1,25(OH)_2D_3$ is strictly controlled dynamic process. At the example of several $1,25(OH)_2D_3$ target genes involved in controlling immune function and cellular growth I could show that chromatin activation, VDR binding and transcriptional activation take place in region- and gene-specific manner. Finally, I indicated that the information from primary $1,25(OH)_2D_3$ target gene expression can be applied to human individuals, in order to evaluate their response to vitamin D_3.

8 References

(1) Hilger J, Friedel A, Herr R, Rausch T, Roos F, Wahl DA, Pierroz DD, Weber P, Hoffmann K. A systematic review of vitamin D status in populations worldwide. Br J Nutr 2014 Jan 14;111(1):23-45.

(2) Suda T, Ueno Y, Fujii K, Shinki T. Vitamin D and bone. J Cell Biochem 2003 Feb 1;88(2):259-266.

(3) Feldman D, Krishnan AV, Swami S, Giovannucci E, Feldman BJ. The role of vitamin D in reducing cancer risk and progression. Nat Rev Cancer 2014 May;14(5):342-357.

(4) Holick MF. Vitamin D deficiency. N Engl J Med 2007 Jul 19;357(3):266-281.

(5) Cashman KD, Kinsella M, McNulty BA, Walton J, Gibney MJ, Flynn A, Kiely M. Dietary vitamin D2 - a potentially underestimated contributor to vitamin D nutritional status of adults? Br J Nutr 2014 Apr 29:1-10.

(6) Jones G, Prosser DE, Kaufmann M. Cytochrome P450-mediated metabolism of vitamin D. J Lipid Res 2014 Jan;55(1):13-31.

(7) Hollis BW. Circulating 25-hydroxyvitamin D levels indicative of vitamin D sufficiency: implications for establishing a new effective dietary intake recommendation for vitamin D. J Nutr 2005 Feb;135(2):317-322.

(8) Institute of Medicine (US). Committee to Review Dietary Reference Intakes for Vitamin D and Calcium. National Academies Press 2011.

(9) Holick MF, Binkley NC, Bischoff-Ferrari HA, Gordon CM, Hanley DA, Heaney RP, Murad MH, Weaver CM, Endocrine Society. Evaluation, treatment, and prevention of vitamin D deficiency: an Endocrine Society clinical practice guideline. J Clin Endocrinol Metab 2011 Jul;96(7):1911-1930.

(10) HUSLAB. The laboratory of Hospital District of Helsinki and Uusimaa, http://huslab.fi/ohjekirja, Accessed 8th of May 2014.

(11) Powe CE, Evans MK, Wenger J, Zonderman AB, Berg AH, Nalls M, Tamez H, Zhang D, Bhan I, Karumanchi SA, Powe NR, Thadhani R. Vitamin D-binding protein and vitamin D status of black Americans and white Americans. N Engl J Med 2013 Nov 21;369(21):1991-2000.

(12) Handel AE, Sandve GK, Disanto G, Berlanga-Taylor AJ, Gallone G, Hanwell H, Drablos F, Giovannoni G, Ebers GC, Ramagopalan SV. Vitamin D receptor ChIP-seq in primary CD4+ cells: relationship to serum 25-hydroxyvitamin D levels and autoimmune disease. BMC Med 2013 Jul 12;11:163-7015-11-163.

(13) Standahl Olsen K, Rylander C, Brustad M, Aksnes L, Lund E. Plasma 25 hydroxyvitamin D level and blood gene expression profiles: a cross-sectional study of the Norwegian Women and Cancer Post-genome Cohort. Eur J Clin Nutr 2013 Jul;67(7):773-778.

(14) Carlberg C, Seuter S, de Mello VD, Schwab U, Voutilainen S, Pulkki K, Nurmi T, Virtanen J, Tuomainen TP, Uusitupa M. Primary vitamin D target genes allow a categorization of possible benefits of vitamin D(3) supplementation. PLoS One 2013 Jul 29;8(7):e71042.

(15) Lindqvist PG, Epstein E, Landin-Olsson M, Ingvar C, Nielsen K, Stenbeck M, Olsson H. Avoidance of sun exposure is a risk factor for all-cause mortality: results from the Melanoma in Southern Sweden cohort. J Intern Med 2014 Apr 4.

(16) Garland CF, Garland FC, Gorham ED, Lipkin M, Newmark H, Mohr SB, Holick MF. The role of vitamin D in cancer prevention. Am J Public Health 2006 Feb;96(2):252-261.

(17) Giovannucci E. Epidemiology of vitamin D and colorectal cancer. Anticancer Agents Med Chem 2013 Jan;13(1):11-19.

(18) Pereira F, Larriba MJ, Munoz A. Vitamin D and colon cancer. Endocr Relat Cancer 2012 May 3;19(3):R51-71.

(19) Grant WB. Update on evidence that support a role of solar ultraviolet-B irradiance in reducing cancer risk. Anticancer Agents Med Chem 2013 Jan;13(1):140-146.

(20) Fang F, Kasperzyk JL, Shui I, Hendrickson W, Hollis BW, Fall K, Ma J, Gaziano JM, Stampfer MJ, Mucci LA, Giovannucci E. Prediagnostic plasma vitamin D metabolites and mortality among patients with prostate cancer. PLoS One 2011 Apr 6;6(4):e18625.

(21) Autier P, Boniol M, Pizot C, Mullie P. Vitamin D status and ill health: a systematic review. Lancet Diabetes Endocrinol 2014 Jan;2(1):76-89.

(22) Lazzeroni M, Serrano D, Pilz S, Gandini S. Vitamin D supplementation and cancer: review of randomized controlled trials. Anticancer Agents Med Chem 2013 Jan;13(1):118-125.

(23) Warfel NA, El-Deiry WS. p21WAF1 and tumourigenesis: 20 years after. Curr Opin Oncol 2013 Jan;25(1):52-58.

(24) Liu M, Lee MH, Cohen M, Bommakanti M, Freedman LP. Transcriptional activation of the Cdk inhibitor p21 by vitamin D3 leads to the induced differentiation of the myelomonocytic cell line U937. Genes Dev 1996 Jan 15;10(2):142-153.

(25) Saramäki A, Banwell CM, Campbell MJ, Carlberg C. Regulation of the human p21(waf1/cip1) gene promoter via multiple binding sites for p53 and the vitamin D3 receptor. Nucleic Acids Res 2006 Jan 24;34(2):543-554.

(26) Verlinden L, Verstuyf A, Convents R, Marcelis S, Van Camp M, Bouillon R. Action of 1,25(OH)2D3 on the cell cycle genes, cyclin D1, p21 and p27 in MCF-7 cells. Mol Cell Endocrinol 1998 Jul 25;142(1-2):57-65.

(27) Wang QM, Jones JB, Studzinski GP. Cyclin-dependent kinase inhibitor p27 as a mediator of the G1-S phase block induced by 1,25-dihydroxyvitamin D3 in HL60 cells. Cancer Res 1996 Jan 15;56(2):264-267.

(28) Huang YC, Hung WC. 1,25-dihydroxyvitamin D3 transcriptionally represses p45Skp2 expression via the Sp1 sites in human prostate cancer cells. J Cell Physiol 2006 Nov;209(2):363-369.

(29) Li P, Li C, Zhao X, Zhang X, Nicosia SV, Bai W. p27(Kip1) stabilization and G(1) arrest by 1,25-dihydroxyvitamin D(3) in ovarian cancer cells mediated through down-regulation of cyclin E/cyclin-dependent kinase 2 and Skp1-Cullin-F-box protein/Skp2 ubiquitin ligase. J Biol Chem 2004 Jun 11;279(24):25260-25267.

(30) Lin R, Wang TT, Miller WH,Jr, White JH. Inhibition of F-Box protein p45(SKP2) expression and stabilization of cyclin-dependent kinase inhibitor p27(KIP1) in vitamin D analog-treated cancer cells. Endocrinology 2003 Mar;144(3):749-753.

(31) Wang X, Gocek E, Liu CG, Studzinski GP. MicroRNAs181 regulate the expression of p27Kip1 in human myeloid leukemia cells induced to differentiate by 1,25-dihydroxyvitamin D3. Cell Cycle 2009 Mar 1;8(5):736-741.

(32) Wade WN, Willingham MC, Koumenis C, Cramer SD. p27Kip1 is essential for the antiproliferative action of 1,25-dihydroxyvitamin D3 in primary, but not immortalized, mouse embryonic fibroblasts. J Biol Chem 2002 Oct 4;277(40):37301-37306.

(33) Flores O, Wang Z, Knudsen KE, Burnstein KL. Nuclear targeting of cyclin-dependent kinase 2 reveals essential roles of cyclin-dependent kinase 2 localization and cyclin E in vitamin D-mediated growth inhibition. Endocrinology 2010 Mar;151(3):896-908.

(34) Brosseau C, Pirianov G, Colston KW. Role of insulin-like growth factor binding protein-3 in 1, 25-dihydroxyvitamin-d 3 -induced breast cancer cell apoptosis. Int J Cell Biol 2013;2013:960378.

(35) Jogie-Brahim S, Feldman D, Oh Y. Unraveling insulin-like growth factor binding protein-3 actions in human disease. Endocr Rev 2009 Aug;30(5):417-437.

(36) Matilainen M, Malinen M, Saavalainen K, Carlberg C. Regulation of multiple insulin-like growth factor binding protein genes by 1 alpha ,25-dihydroxyvitamin D sub(3). Nucleic Acids Res 2005;33(17):5521-5532.

(37) Blutt SE, McDonnell TJ, Polek TC, Weigel NL. Calcitriol-induced apoptosis in LNCaP cells is blocked by overexpression of Bcl-2. Endocrinology 2000 Jan;141(1):10-17.

(38) Mathiasen IS, Lademann U, Jäättelä M. Apoptosis induced by vitamin D compounds in breast cancer cells is inhibited by Bcl-2 but does not involve known caspases or p53. Cancer research 1999 Oct 1;59(19):4848-4856.

(39) Schwende H, Fitzke E, Ambs P, Dieter P. Differences in the state of differentiation of THP-1 cells induced by phorbol ester and 1,25-dihydroxyvitamin D3. J Leukoc Biol 1996 Apr;59(4):555-561.

(40) Gocek E, Studzinski GP. Vitamin D and differentiation in cancer. Crit Rev Clin Lab Sci 2009;46(4):190-209.

(41) Larriba MJ, Gonzalez-Sancho JM, Bonilla F, Munoz A. Interaction of vitamin D with membrane-based signaling pathways. Front Physiol 2014 Feb 18;5:60.

(42) Palmer HG, Gonzalez-Sancho JM, Espada J, Berciano MT, Puig I, Baulida J, Quintanilla M, Cano A, de Herreros AG, Lafarga M, Munoz A. Vitamin D(3) promotes the differentiation of colon carcinoma cells by the induction of E-cadherin and the inhibition of beta-catenin signaling. J Cell Biol 2001 Jul 23;154(2):369-387.

(43) Aguilera O, Pena C, Garcia JM, Larriba MJ, Ordonez-Moran P, Navarro D, Barbachano A, Lopez de Silanes I, Ballestar E, Fraga MF, Esteller M, Gamallo C, Bonilla F, Gonzalez-Sancho JM, Munoz A. The Wnt antagonist DICKKOPF-1 gene is induced by 1alpha,25-dihydroxyvitamin D3 associated to the differentiation of human colon cancer cells. Carcinogenesis 2007 Sep;28(9):1877-1884.

(44) Baeke F, Takiishi T, Korf H, Gysemans C, Mathieu C. Vitamin D: modulator of the immune system. Curr Opin Pharmacol 2010 Aug;10(4):482-496.

(45) Provvedini DM, Tsoukas CD, Deftos LJ, Manolagas SC. 1,25-dihydroxyvitamin D3 receptors in human leukocytes. Science 1983 Sep 16;221(4616):1181-1183.

(46) Veldman CM, Cantorna MT, DeLuca HF. Expression of 1,25-dihydroxyvitamin D(3) receptor in the immune system. Arch Biochem Biophys 2000 Feb 15;374(2):334-338.

(47) Sadeghi K, Wessner B, Laggner U, Ploder M, Tamandl D, Friedl J, Zugel U, Steinmeyer A, Pollak A, Roth E, Boltz-Nitulescu G, Spittler A. Vitamin D3 down-regulates monocyte TLR expression and triggers hyporesponsiveness to pathogen-associated molecular patterns. Eur J Immunol 2006 Feb;36(2):361-370.

(48) Cohen-Lahav M, Shany S, Tobvin D, Chaimovitz C, Douvdevani A. Vitamin D decreases NFkappaB activity by increasing IkappaBalpha levels. Nephrol Dial Transplant 2006 Apr;21(4):889-897.

(49) Harant H, Wolff B, Lindley IJ. 1Alpha,25-dihydroxyvitamin D3 decreases DNA binding of nuclear factor-kappaB in human fibroblasts. FEBS Lett 1998 Oct 9;436(3):329-334.

(50) Matilainen JM, Husso T, Toropainen S, Seuter S, Turunen MP, Gynther P, Ylä-Herttuala S, Carlberg C, Väisänen S. Primary effect of 1alpha,25(OH)(2)D(3) on IL-10

expression in monocytes is short-term down-regulation. Biochim Biophys Acta 2010 Nov;1803(11):1276-1286.

(51) Matilainen JM, Räsänen A, Gynther P, Väisänen S. The genes encoding cytokines IL-2, IL-10 and IL-12B are primary 1alpha,25(OH)2D3 target genes. J Steroid Biochem Mol Biol 2010 Jul;121(1-2):142-145.

(52) O'Garra A, Vieira P. T(H)1 cells control themselves by producing interleukin-10. Nat Rev Immunol 2007 Jun;7(6):425-428.

(53) Verway M, Bouttier M, Wang TT, Carrier M, Calderon M, An BS, Devemy E, McIntosh F, Divangahi M, Behr MA, White JH. Vitamin D induces interleukin-1beta expression: paracrine macrophage epithelial signaling controls M. tuberculosis infection. PLoS Pathog 2013;9(6):e1003407.

(54) Giulietti A, van Etten E, Overbergh L, Stoffels K, Bouillon R, Mathieu C. Monocytes from type 2 diabetic patients have a pro-inflammatory profile. 1,25-Dihydroxyvitamin D(3) works as anti-inflammatory. Diabetes Res Clin Pract 2007 Jul;77(1):47-57.

(55) Vimaleswaran KS, Berry DJ, Lu C, Tikkanen E, Pilz S, Hiraki LT, Cooper JD, Dastani Z, Li R, Houston DK, et al. Causal relationship between obesity and vitamin D status: bi-directional Mendelian randomization analysis of multiple cohorts. PLoS Med 2013;10(2):e1001383.

(56) Wortsman J, Matsuoka LY, Chen TC, Lu Z, Holick MF. Decreased bioavailability of vitamin D in obesity. Am J Clin Nutr 2000 Sep;72(3):690-693.

(57) Drincic AT, Armas LA, Van Diest EE, Heaney RP. Volumetric dilution, rather than sequestration best explains the low vitamin D status of obesity. Obesity (Silver Spring) 2012 Jul;20(7):1444-1448.

(58) Sun X, Morris KL, Zemel MB. Role of calcitriol and cortisol on human adipocyte proliferation and oxidative and inflammatory stress: a microarray study. J Nutrigenet Nutrigenomics 2008;1(1-2):30-48.

(59) Trayhurn P, O'Hara A, Bing C. Interrogation of microarray datasets indicates that macrophage-secreted factors stimulate the expression of genes associated with vitamin D metabolism (VDR and CYP27B1) in human adipocytes. Adipobiology 2011;3:31-36.

(60) Mutt SJ, Karhu T, Lehtonen S, Lehenkari P, Carlberg C, Saarnio J, Sebert S, Hyppönen E, Järvelin MR, Herzig KH. Inhibition of cytokine secretion from adipocytes by 1,25-dihydroxyvitamin D(3) via the NF-kappaB pathway. FASEB J 2012 Nov;26(11):4400-4407.

(61) Gao D, Trayhurn P, Bing C. 1,25-Dihydroxyvitamin D3 inhibits the cytokine-induced secretion of MCP-1 and reduces monocyte recruitment by human preadipocytes. Int J Obes (Lond) 2013 Mar;37(3):357-365.

(62) Lahnalampi M, Heinäniemi M, Sinkkonen L, Wabitsch M, Carlberg C. Time-resolved expression profiling of the nuclear receptor superfamily in human adipogenesis. PLoS One 2010 Sep 27;5(9):e12991.

(63) Carlberg C, Molnar F. Current status of vitamin D signaling and its therapeutic applications. Curr Top Med Chem 2012;12(6):528-547.

(64) Wang Y, Zhu J, DeLuca HF. Where is the vitamin D receptor? Arch Biochem Biophys 2012 Jul 1;523(1):123-133.

(65) Mangelsdorf DJ, Thummel C, Beato M, Herrlich P, Schutz G, Umesono K, Blumberg B, Kastner P, Mark M, Chambon P, Evans RM. The nuclear receptor superfamily: the second decade. Cell 1995 Dec 15;83(6):835-839.

(66) Orlov I, Rochel N, Moras D, Klaholz BP. Structure of the full human RXR/VDR nuclear receptor heterodimer complex with its DR3 target DNA. EMBO J 2012 Jan 18;31(2):291-300.

(67) Nagy L, Schwabe JW. Mechanism of the nuclear receptor molecular switch. Trends Biochem Sci 2004 Jun;29(6):317-324.

(68) Carlberg C, Bendik I, Wyss A, Meier E, Sturzenbecker LJ, Grippo JF, Hunziker W. Two nuclear signalling pathways for vitamin D. Nature 1993 Feb 18;361(6413):657-660.

(69) Umesono K, Murakami KK, Thompson CC, Evans RM. Direct repeats as selective response elements for the thyroid hormone, retinoic acid, and vitamin D3 receptors. Cell 1991 Jun 28;65(7):1255-1266.

(70) Prufer K, Racz A, Lin GC, Barsony J. Dimerization with retinoid X receptors promotes nuclear localization and subnuclear targeting of vitamin D receptors. J Biol Chem 2000 Dec 29;275(52):41114-41123.

(71) Tuoresmäki P, Väisänen S, Neme A, Heikkinen S, Carlberg C. Patterns of Genome-Wide VDR Locations. PLoS One 2014 Apr 30;9(4):e96105.

(72) Polly P, Herdick M, Moehren U, Baniahmad A, Heinzel T, Carlberg C. VDR-Alien: a novel, DNA-selective vitamin D(3) receptor-corepressor partnership. FASEB J 2000 Jul;14(10):1455-1463.

(73) Privalsky ML. The role of corepressors in transcriptional regulation by nuclear hormone receptors. Annu Rev Physiol 2004;66:315-360.

(74) Carlberg C, Campbell MJ. Vitamin D receptor signaling mechanisms: integrated actions of a well-defined transcription factor. Steroids 2013 Feb;78(2):127-136.

(75) Gronemeyer H, Gustafsson JA, Laudet V. Principles for modulation of the nuclear receptor superfamily. Nat Rev Drug Discov 2004 Nov;3(11):950-964.

(76) Saramäki A, Diermeier S, Kellner R, Laitinen H, Väisänen S, Carlberg C. Cyclical chromatin looping and transcription factor association on the regulatory regions of the

p21 (CDKN1A) gene in response to 1alpha,25-dihydroxyvitamin D3. J Biol Chem 2009 Mar 20;284(12):8073-8082.

(77) Metivier R, Penot G, Hubner MR, Reid G, Brand H, Kos M, Gannon F. Estrogen receptor-alpha directs ordered, cyclical, and combinatorial recruitment of cofactors on a natural target promoter. Cell 2003 Dec 12;115(6):751-763.

(78) Kim S, Shevde NK, Pike JW. 1,25-Dihydroxyvitamin D3 stimulates cyclic vitamin D receptor/retinoid X receptor DNA-binding, co-activator recruitment, and histone acetylation in intact osteoblasts. J Bone Miner Res 2005 Feb;20(2):305-317.

(79) Väisänen S, Dunlop TW, Sinkkonen L, Frank C, Carlberg C. Spatio-temporal activation of chromatin on the human CYP24 gene promoter in the presence of 1alpha,25-Dihydroxyvitamin D3. J Mol Biol 2005 Jul 1;350(1):65-77.

(80) Carlberg C, Seuter S. Dynamics of nuclear receptor target gene regulation. Chromosoma 2010 Oct;119(5):479-484.

(81) Heikkinen S, Väisänen S, Pehkonen P, Seuter S, Benes V, Carlberg C. Nuclear hormone 1alpha,25-dihydroxyvitamin D3 elicits a genome-wide shift in the locations of VDR chromatin occupancy. Nucleic Acids Res 2011 Nov;39(21):9181-9193.

(82) Ramagopalan SV, Heger A, Berlanga AJ, Maugeri NJ, Lincoln MR, Burrell A, Handunnetthi L, Handel AE, Disanto G, Orton SM, et al. A ChIP-seq defined genome-wide map of vitamin D receptor binding: associations with disease and evolution. Genome Res 2010 Oct;20(10):1352-1360.

(83) Ding N, Yu RT, Subramaniam N, Sherman MH, Wilson C, Rao R, Leblanc M, Coulter S, He M, Scott C, et al. A vitamin D receptor/SMAD genomic circuit gates hepatic fibrotic response. Cell 2013 Apr 25;153(3):601-613.

(84) Meyer MB, Goetsch PD, Pike JW. VDR/RXR and TCF4/beta-catenin cistromes in colonic cells of colorectal tumor origin: impact on c-FOS and c-MYC gene expression. Mol Endocrinol 2012 Jan;26(1):37-51.

(85) Eberharter A, Becker PB. Histone acetylation: a switch between repressive and permissive chromatin. Second in review series on chromatin dynamics. EMBO Rep 2002 Mar;3(3):224-229.

(86) Seuter S, Pehkonen P, Heikkinen S, Carlberg C. Dynamics of 1alpha,25-dihydroxyvitamin D3-dependent chromatin accessibility of early vitamin D receptor target genes. Biochim Biophys Acta 2013 Dec;1829(12):1266-1275.

(87) Jones JI, Clemmons DR. Insulin-like growth factors and their binding proteins: biological actions. Endocr Rev 1995 Feb;16(1):3-34.

(88) Hwa V, Oh Y, Rosenfeld RG. The insulin-like growth factor-binding protein (IGFBP) superfamily. Endocrine reviews 1999 Dec;20(6):761-787.

(89) Martin JL, Baxter RC. Signalling pathways of insulin-like growth factors (IGFs) and IGF binding protein-3. Growth Factors 2011 Dec;29(6):235-244.

(90) Colston KW, Perks CM, Xie SP, Holly JM. Growth inhibition of both MCF-7 and Hs578T human breast cancer cell lines by vitamin D analogues is associated with increased expression of insulin-like growth factor binding protein-3. J Mol Endocrinol 1998 Feb;20(1):157-162.

(91) Liu B, Lee H, Weinzimer S, Powell D, Clifford J, Kurie J, Cohen P. Direct Functional Interactions between Insulin-like Growth Factor-binding Protein-3 and Retinoid X Receptor- alpha Regulate Transcriptional Signaling and Apoptosis. J Biol Chem 2000 27 Oct;275(43):33607-33613.

(92) Boyle BJ, Zhao XY, Cohen P, Feldman D. Insulin-like growth factor binding protein-3 mediates 1 alpha,25-dihydroxyvitamin d(3) growth inhibition in the LNCaP prostate cancer cell line through p21/WAF1. The Journal of urology 2001 Apr;165(4):1319-1324.

(93) Peng L, Malloy PJ, Feldman D. Identification of a functional vitamin D response element in the human insulin-like growth factor binding protein-3 promoter. Molecular endocrinology (Baltimore, Md) 2004 May;18(5):1109-1119.

(94) Russell L, Forsdyke DR. A human putative lymphocyte G0/G1 switch gene containing a CpG-rich island encodes a small basic protein with the potential to be phosphorylated. DNA Cell Biol 1991 Oct;10(8):581-591.

(95) Yamada T, Park CS, Shen Y, Rabin KR, Lacorazza HD. G0S2 inhibits the proliferation of K562 cells by interacting with nucleolin in the cytosol. Leuk Res 2014 Feb;38(2):210-217.

(96) Heckmann BL, Zhang X, Xie X, Liu J. The G0/G1 switch gene 2 (G0S2): regulating metabolism and beyond. Biochim Biophys Acta 2013 Feb;1831(2):276-281.

(97) Yamada T, Park CS, Burns A, Nakada D, Lacorazza HD. The cytosolic protein G0S2 maintains quiescence in hematopoietic stem cells. PLoS One 2012;7(5):e38280.

(98) Zandbergen F, Mandard S, Escher P, Tan NS, Patsouris D, Jatkoe T, Rojas-Caro S, Madore S, Wahli W, Tafuri S, Muller M, Kersten S. The G0/G1 switch gene 2 is a novel PPAR target gene. Biochem J 2005 Dec 1;392(Pt 2):313-324.

(99) Kriebitzsch C, Verlinden L, Eelen G, Tan BK, Van Camp M, Bouillon R, Verstuyf A. The impact of 1,25(OH)2D3 and its structural analogs on gene expression in cancer cells--a microarray approach. Anticancer Res 2009 Sep;29(9):3471-3483.

(100) Singh PK, Doig CL, Dhiman VK, Turner BM, Smiraglia DJ, Campbell MJ. Epigenetic distortion to VDR transcriptional regulation in prostate cancer cells. J Steroid Biochem Mol Biol 2013 Jul;136:258-263.

(101) Srivastava M, Pollard HB. Molecular dissection of nucleolin's role in growth and cell proliferation: new insights. FASEB J 1999 Nov;13(14):1911-1922.

(102) el-Deiry WS, Tokino T, Velculescu VE, Levy DB, Parsons R, Trent JM, Lin D, Mercer WE, Kinzler KW, Vogelstein B. WAF1, a potential mediator of p53 tumor suppression. Cell 1993 Nov 19;75(4):817-825.

(103) Rao A, Coan A, Welsh JE, Barclay WW, Koumenis C, Cramer SD. Vitamin D receptor and p21/WAF1 are targets of genistein and 1,25-dihydroxyvitamin D3 in human prostate cancer cells. Cancer Res 2004 Mar 15;64(6):2143-2147.

(104) Cheng M, Olivier P, Diehl JA, Fero M, Roussel MF, Roberts JM, Sherr CJ. The p21(Cip1) and p27(Kip1) CDK 'inhibitors' are essential activators of cyclin D-dependent kinases in murine fibroblasts. EMBO J 1999 Mar 15;18(6):1571-1583.

(105) Waga S, Hannon GJ, Beach D, Stillman B. The p21 inhibitor of cyclin-dependent kinases controls DNA replication by interaction with PCNA. Nature 1994 Jun 16;369(6481):574-578.

(106) Kitaura H, Shinshi M, Uchikoshi Y, Ono T, Iguchi-Ariga SM, Ariga H. Reciprocal regulation via protein-protein interaction between c-Myc and p21(cip1/waf1/sdi1) in DNA replication and transcription. J Biol Chem 2000 Apr 7;275(14):10477-10483.

(107) Baptiste-Okoh N, Barsotti AM, Prives C. Caspase 2 is both required for p53-mediated apoptosis and downregulated by p53 in a p21-dependent manner. Cell Cycle 2008 May 1;7(9):1133-1138.

(108) Jin YH, Yoo KJ, Lee YH, Lee SK. Caspase 3-mediated cleavage of p21WAF1/CIP1 associated with the cyclin A-cyclin-dependent kinase 2 complex is a prerequisite for apoptosis in SK-HEP-1 cells. J Biol Chem 2000 Sep 29;275(39):30256-30263.

(109) Paramio JM, Segrelles C, Ruiz S, Martin-Caballero J, Page A, Martinez J, Serrano M, Jorcano JL. The ink4a/arf tumor suppressors cooperate with p21cip1/waf in the processes of mouse epidermal differentiation, senescence, and carcinogenesis. J Biol Chem 2001 Nov 23;276(47):44203-44211.

(110) Jackson RJ, Engelman RW, Coppola D, Cantor AB, Wharton W, Pledger WJ. p21Cip1 nullizygosity increases tumor metastasis in irradiated mice. Cancer Res 2003 Jun 15;63(12):3021-3025.

(111) Abbas T, Dutta A. P21 in Cancer: Intricate Networks and Multiple Activities. Nat Rev Cancer 2009 Jun;9(6):400-414.

(112) Zhou BP, Liao Y, Xia W, Spohn B, Lee MH, Hung MC. Cytoplasmic localization of p21Cip1/WAF1 by Akt-induced phosphorylation in HER-2/neu-overexpressing cells. Nat Cell Biol 2001 Mar;3(3):245-252.

(113) Cowling VH, Cole MD. Mechanism of transcriptional activation by the Myc oncoproteins. Semin Cancer Biol 2006 Aug;16(4):242-252.

(114) Cole MD, Cowling VH. Transcription-independent functions of MYC: regulation of translation and DNA replication. Nat Rev Mol Cell Biol 2008 Oct;9(10):810-815.

(115) Dang CV, O'Donnell KA, Zeller KI, Nguyen T, Osthus RC, Li F. The c-Myc target gene network. Semin Cancer Biol 2006 Aug;16(4):253-264.

(116) Rahl PB, Lin CY, Seila AC, Flynn RA, McCuine S, Burge CB, Sharp PA, Young RA. c-Myc regulates transcriptional pause release. Cell 2010 Apr 30;141(3):432-445.

(117) Perna D, Faga G, Verrecchia A, Gorski MM, Barozzi I, Narang V, Khng J, Lim KC, Sung WK, Sanges R, et al. Genome-wide mapping of Myc binding and gene regulation in serum-stimulated fibroblasts. Oncogene 2012 Mar 29;31(13):1695-1709.

(118) Zeller KI, Zhao X, Lee CW, Chiu KP, Yao F, Yustein JT, Ooi HS, Orlov YL, Shahab A, Yong HC, et al. Global mapping of c-Myc binding sites and target gene networks in human B cells. Proc Natl Acad Sci U S A 2006 Nov 21;103(47):17834-17839.

(119) Dominguez-Sola D, Ying CY, Grandori C, Ruggiero L, Chen B, Li M, Galloway DA, Gu W, Gautier J, Dalla-Favera R. Non-transcriptional control of DNA replication by c-Myc. Nature 2007 Jul 26;448(7152):445-451.

(120) Beroukhim R, Mermel CH, Porter D, Wei G, Raychaudhuri S, Donovan J, Barretina J, Boehm JS, Dobson J, Urashima M, et al. The landscape of somatic copy-number alteration across human cancers. Nature 2010 Feb 18;463(7283):899-905.

(121) Soucek L, Whitfield J, Martins CP, Finch AJ, Murphy DJ, Sodir NM, Karnezis AN, Swigart LB, Nasi S, Evan GI. Modelling Myc inhibition as a cancer therapy. Nature 2008 Oct 2;455(7213):679-683.

(122) Reitsma PH, Rothberg PG, Astrin SM, Trial J, Bar-Shavit Z, Hall A, Teitelbaum SL, Kahn AJ. Regulation of myc gene expression in HL-60 leukaemia cells by a vitamin D metabolite. Nature 1983 Dec 1-7;306(5942):492-494.

(123) Toropainen S, Väisänen S, Heikkinen S, Carlberg C. The down-regulation of the human MYC gene by the nuclear hormone 1alpha,25-dihydroxyvitamin D3 is associated with cycling of corepressors and histone deacetylases. J Mol Biol 2010 Jul 16;400(3):284-294.

(124) Van Damme J, Van Beeumen J, Opdenakker G, Billiau A. A novel, NH2-terminal sequence-characterized human monokine possessing neutrophil chemotactic, skin-reactive, and granulocytosis-promoting activity. J Exp Med 1988 Apr 1;167(4):1364-1376.

(125) Zlotnik A, Yoshie O. The chemokine superfamily revisited. Immunity 2012 May 25;36(5):705-716.

(126) Moser B, Wolf M, Walz A, Loetscher P. Chemokines: multiple levels of leukocyte migration control. Trends Immunol 2004 Feb;25(2):75-84.

(127) Flad HD, Brandt E. Platelet-derived chemokines: pathophysiology and therapeutic aspects. Cell Mol Life Sci 2010 Jul;67(14):2363-2386.

(128) Nomiyama H, Osada N, Yoshie O. The evolution of mammalian chemokine genes. Cytokine Growth Factor Rev 2010 Aug;21(4):253-262.

(129) Kiefer F, Siekmann AF. The role of chemokines and their receptors in angiogenesis. Cell Mol Life Sci 2011 Sep;68(17):2811-2830.

(130) Mortier A, Berghmans N, Ronsse I, Grauwen K, Stegen S, Van Damme J, Proost P. Biological activity of CXCL8 forms generated by alternative cleavage of the signal peptide or by aminopeptidase-mediated truncation. PLoS One 2011;6(8):e23913.

(131) Vandercappellen J, Van Damme J, Struyf S. The role of CXC chemokines and their receptors in cancer. Cancer Lett 2008 Aug 28;267(2):226-244.

(132) Nasser MW, Raghuwanshi SK, Grant DJ, Jala VR, Rajarathnam K, Richardson RM. Differential activation and regulation of CXCR1 and CXCR2 by CXCL8 monomer and dimer. J Immunol 2009 Sep 1;183(5):3425-3432.

(133) Hoffmann E, Dittrich-Breiholz O, Holtmann H, Kracht M. Multiple control of interleukin-8 gene expression. J Leukoc Biol 2002 Nov;72(5):847-855.

(134) Andreev J, Simon JP, Sabatini DD, Kam J, Plowman G, Randazzo PA, Schlessinger J. Identification of a new Pyk2 target protein with Arf-GAP activity. Mol Cell Biol 1999 Mar;19(3):2338-2350.

(135) Hashimoto S, Hashimoto A, Yamada A, Kojima C, Yamamoto H, Tsutsumi T, Higashi M, Mizoguchi A, Yagi R, Sabe H. A novel mode of action of an ArfGAP, AMAP2/PAG3/Papa lpha, in Arf6 function. J Biol Chem 2004 Sep 3;279(36):37677-37684.

(136) Uchida H, Kondo A, Yoshimura Y, Mazaki Y, Sabe H. PAG3/Papalpha/KIAA0400, a GTPase-activating protein for ADP-ribosylation factor (ARF), regulates ARF6 in Fcgamma receptor-mediated phagocytosis of macrophages. J Exp Med 2001 Apr 16;193(8):955-966.

(137) Soule HD, Maloney TM, Wolman SR, Peterson WD,Jr, Brenz R, McGrath CM, Russo J, Pauley RJ, Jones RF, Brooks SC. Isolation and characterization of a spontaneously immortalized human breast epithelial cell line, MCF-10. Cancer Res 1990 Sep 15;50(18):6075-6086.

(138) Bello D, Webber MM, Kleinman HK, Wartinger DD, Rhim JS. Androgen responsive adult human prostatic epithelial cell lines immortalized by human papillomavirus 18. Carcinogenesis 1997 Jun;18(6):1215-1223.

(139) Tsuchiya S, Yamabe M, Yamaguchi Y, Kobayashi Y, Konno T, Tada K. Establishment and characterization of a human acute monocytic leukemia cell line (THP-1). Int J Cancer 1980 Aug;26(2):171-176.

(140) Wabitsch M, Brenner RE, Melzner I, Braun M, Moller P, Heinze E, Debatin KM, Hauner H. Characterization of a human preadipocyte cell strain with high capacity for adipose differentiation. Int J Obes Relat Metab Disord 2001 Jan;25(1):8-15.

(141) Nurmi T, Tuomainen TP, Virtanen J, Mursu J, Voutilainen S. High-performance liquid chromatography and coulometric electrode array detector in serum 25-hydroxyvitamin D(3) and 25-hydroxyvitamin D(2) analyses. Anal Biochem 2013 Apr 1;435(1):1-9.

(142) ENCODE Project Consortium, Bernstein BE, Birney E, Dunham I, Green ED, Gunter C, Snyder M. An integrated encyclopedia of DNA elements in the human genome. Nature 2012 Sep 6;489(7414):57-74.

(143) Thorvaldsdottir H, Robinson JT, Mesirov JP. Integrative Genomics Viewer (IGV): high-performance genomics data visualization and exploration. Brief Bioinform 2013 Mar;14(2):178-192.

(144) Kent WJ, Sugnet CW, Furey TS, Roskin KM, Pringle TH, Zahler AM, Haussler D. The human genome browser at UCSC. Genome Res 2002 Jun;12(6):996-1006.

(145) Phillips JE, Corces VG. CTCF: master weaver of the genome. Cell 2009 Jun 26;137(7):1194-1211.

(146) Schmidt D, Schwalie PC, Wilson MD, Ballester B, Goncalves A, Kutter C, Brown GD, Marshall A, Flicek P, Odom DT. Waves of retrotransposon expansion remodel genome organization and CTCF binding in multiple mammalian lineages. Cell 2012 Jan 20;148(1-2):335-348.

(147) Klein E, Ben-Bassat H, Neumann H, Ralph P, Zeuthen J, Polliack A, Vanky F. Properties of the K562 cell line, derived from a patient with chronic myeloid leukemia. Int J Cancer 1976 Oct 15;18(4):421-431.

(148) Sur I, Tuupanen S, Whitington T, Aaltonen LA, Taipale J. Lessons from functional analysis of genome-wide association studies. Cancer Res 2013 Jul 15;73(14):4180-4184.

(149) Conway EM. Thrombomodulin and its role in inflammation. Semin Immunopathol 2012 Jan;34(1):107-125.

(150) Iyer SP, Akimoto Y, Hart GW. Identification and cloning of a novel family of coiled-coil domain proteins that interact with O-GlcNAc transferase. J Biol Chem 2003 Feb 14;278(7):5399-5409.

(151) Dickinson RJ, Keyse SM. Diverse physiological functions for dual-specificity MAP kinase phosphatases. J Cell Sci 2006 Nov 15;119(Pt 22):4607-4615.

(152) Nautiyal J, Christian M, Parker MG. Distinct functions for RIP140 in development, inflammation, and metabolism. Trends Endocrinol Metab 2013 Sep;24(9):451-459.

Jussi Ryynänen

Pleiotropy of Vitamin D-Mediated Gene Regulation

Vitamin D is an important regulator of gene expression. Epidemiological evidence suggests a protective role of vitamin D against various diseases. Therefore, the molecular basis of vitamin D signaling needs to be elucidated. This thesis investigated the regulation of key vitamin D target genes, in order to provide further insight into the role of vitamin D in cancer and immunity. In this context it was found that certain vitamin D target genes can be used as biomarkers for the vitamin D status of human individuals.

UNIVERSITY OF EASTERN FINLAND

Publications of the University of Eastern Finland

Dissertations in Health Sciences

ISBN 978-952-61-1495-8